Size and body condition drive the energetic cost of a baleen whale foraging in shallow habitat

Clara N. Bird[1], Enrico Pirotta[2], Leslie New[3], Jamie M. Cornelius[4], James L. Sumich[5], Kate M. Colson[1,6], K.C. Bierlich[1], Lisa Hildebrand[1], Alejandro Apolo Fernández Ajó[1], Annie Doron[1,7] and Leigh G. Torres[1]

[1] Geospatial Ecology of Marine Megafauna Lab, Marine Mammal Institute, Department of Fisheries, Wildlife and Conservation Sciences, Oregon State University, Newport, OR, United States of America
[2] Centre for Research into Ecological and Environmental Modelling, University of St Andrews, St Andrews, United Kingdom
[3] Ursinus College, Collegeville, PA, United States of America
[4] Integrative Biology, Oregon State University, Corvallis, OR, United States of America
[5] Marine Mammal Institute, Department of Fisheries, Wildlife and Conservation Sciences, Oregon Statec University, Corvallis, OR, United States of America
[6] Marine Mammal Research Unit, Institute for the Oceans and Fisheries, University of British Columbia, Vancouver, British Columbia, Canada
[7] University of Sheffield, Sheffield, United Kingdom

ABSTRACT

Energy expenditure strongly influences an animal's foraging decisions and activity budgets. Diving animals especially need to be energetically efficient because they exercise while oxygen is limited. By estimating the energetics of behavior, we can better understand the cascading effects of individual responses to disturbance and environmental change. Pacific Coast Feeding Group (PCFG) gray whales use a variety of foraging tactics in shallow habitats (<20 m), which present challenges associated with maneuverability and buoyancy. We use a seven-year dataset of concurrent individual behavior, morphology, and breath-by-breath respiration data collected via drone paired with two years of tri-axial accelerometry tag data to study patterns and correlates of respiration. We assess how several respiration metrics (acting as proxies for oxygen consumption) are associated with individual length, body condition and behavior (forage and travel), and test whether respiration reflects recovery from, or anticipation of, a foraging dive using Bayesian linear mixed effects models. Given model results, we simulated daily field metabolic rate (FMR) to explore how diving costs may affect energetics at a daily scale. We find that respiration reflects recovery from the preceding dive and that dives are more energetically expensive for longer, more buoyant whales. Longer dives and the most common foraging tactics also incur higher energetic costs. FMR simulations show that individual size and dive duration have the largest effects on energy expenditure. Thus, PCFG gray whale foraging success may be limited by the energetic costs associated with size and buoyancy, highlighting the costs of a shallow habitat foraging niche.

Subjects Animal Behavior, Ecology, Marine Biology, Zoology

Keywords PCFG gray whales, Respiration physiology, Bayesian linear mixed effects models, Behavior, Diving, Drones, Biotelemetry

Submitted 21 April 2025
Accepted 25 September 2025
Published 30 October 2025

Corresponding author
Clara N. Bird,
clara.bird@oregonstate.edu,
clara.birdferrer@gmail.com

Academic editor
Eric Ward

Additional Information and Declarations can be found on page 26

DOI **10.7717/peerj.20247**

How to cite this article Bird CN, Pirotta E, New L, Cornelius JM, Sumich JL, Colson KM, Bierlich KC, Hildebrand L, Fernández Ajó AA, Doron A, Torres LG. 2025. Size and body condition drive the energetic cost of a baleen whale foraging in shallow habitat. *PeerJ* **13**:e20247
http://doi.org/10.7717/peerj.20247

INTRODUCTION

An individual's activity and energetic budgets are fundamentally linked, as locomotion requires energy. Measuring both behavior and energy expenditure in tandem can inform the causes and consequences of an individual's decisions, such as resource or space use (*Brown et al., 2004*). In the context of foraging, when animals are both gaining and spending energy, the profitability of different prey types depends on their energetic value and the energetic cost of pursuing, capturing, and handling the prey (*Emlen, 1966*; *Schoener, 1971*). In turn, understanding foraging energetics and decision-making can support conservation efforts, particularly through studies of how behavioral responses to disturbance could scale to population-level impact (*Cooke et al., 2014*; *Pirotta et al., 2018*). However, measuring energy expenditure in wild animals can be challenging and often involves proxy measures of metabolic rate.

Air-breathing, diving animals, including cetaceans, are among the most challenging animals to study behavior and energy expenditure, as they often expend most energy during dives while submerged and oxygen limited (*Irving, 1939*). Given the need for oxygen, the ocean's surface can be considered a central place and dives can be studied within the framework of central place foraging theory (*Doniol-Valcroze et al., 2011*); animals have a limited amount of time before they must return the surface. Consequently, efficient use of oxygen primarily determines the accessibility and profitability of prey (*Houston & McNamara, 1985*). Accordingly, diving animals have several adaptations to efficiently store and use oxygen during apneic periods (*Scholander, 1940*; *Kooyman & Ponganis, 1998*).

Oxygen stores vary between species due to differences in body size, dive behavior, and physiology (*Scholander, 1940*; *Cartwright et al., 2016*). Both oxygen stores (*Kooyman, 1973*; *Noren & Williams, 2000*; *Sumich & May, 2009*) and consumption (*Kleiber, 1975*; *He et al., 2023*) allometrically scale with body size, though by different factors. The energetic cost of a dive also depends on more dynamic variables, as differing levels of exercise associated with activity state and buoyancy affect oxygen use (*Williams et al., 2015*; *Ponganis & Williams, 2016*).

Oxygen acquisition in between consecutive dives has been associated with both recovery from and anticipation for dives (*Ridgway, Scronce & Kanwisher, 1969*; *Isojunno et al., 2018*). Measures of surface duration, heart rate, breath count, oxygen acquisition, and respiration rate during recovery surfacings indicate that longer dives cost more energy (*Kooyman, 1973*; *Dolphin, 1987a*; *Keen & Qualls, 2018*), though this energetic cost also varies across behavior states and travel speeds (*Butler & Woakes, 1979*; *Sumich, 1983*; *Dolphin, 1987b*; *McRae et al., 2024*; *Spina et al., 2024*). Respiration patterns associated with anticipation for a dive include hyperventilation (*Ridgway, Scronce & Kanwisher, 1969*; *Dolphin, 1987a*) and longer terminal breath durations (*Nazario et al., 2022*). Respiration at the surface can also reflect recovery from oxygen-debt accumulation or delayed carbon dioxide removal across multiple dives (*Fahlman et al., 2008a*; *Génin et al., 2015*). Deeper dives are generally thought to be more energetically expensive as they tend be longer than shallow dives (*Doniol-Valcroze et al., 2011*), but deep divers can use buoyancy to their advantage by gliding to reduce energetic costs (*Williams, 1999*). In contrast, buoyancy only increases

the cost of shallow dives (*Kooyman, 1973*; *Stephenson et al., 1989*; *Lovvorn & Jones, 1991*). Therefore, while the dive physiology of deep divers is well studied, the adaptations and costs associated with shallow divers are less understood.

Respiration metrics can serve as accessible proxies for oxygen consumption (*i.e.,* energetic expenditure; *Scholander, 1940*). While respirometry provides the most direct measures of oxygen consumption, it requires handling (*Olsen, Hale & Elsner, 1969*; *Sumich, 2001*; *Fahlman et al., 2008a*), which is infeasible, impractical, or unethical for most cetaceans. Surface ventilation patterns of wild cetaceans can be measured non-invasively (*e.g.*, respiration rate, inter-breath interval, surface duration; *Sumich, 1983*; *Dolphin, 1987a*; *Dolphin, 1987b*; *Stelle, Megill & Kinzel, 2008*; *Williams & Noren, 2009*; *Christiansen, Rasmussen & Lusseau, 2014*; *Keen & Qualls, 2018*). However, converting these remotely measured variables into consumed oxygen relies on assumptions around the tidal volume (*i.e.,* the amount of air exchanged with each respiratory cycle) and oxygen extraction efficiencies (*Fahlman et al., 2016*), which can introduce high uncertainty (*Winship, Trites & Rosen, 2002*).

Relative to all other baleen whales, gray whales (*Eschrichtius robustus*) have a rich history of respiration studies, making them an excellent species for estimating energetic expenditure based on respiration metrics. Respirometry studies on gray whale calves, both restrained and in human care, have quantified oxygen extraction efficiency, flow rate, inhalation and exhalation durations, and tidal volume (*Wahrenbrock et al., 1974*; *Kooyman, Norris & Gentry, 1975*; *Sumich, 2001*). These studies found that, in a single breath, the inhalation and exhalation durations were equal, flow rate peaked halfway through an inhalation or exhalation, oxygen extraction efficiency increased with inhalation duration, and tidal volume can be accurately estimated from body length and inhalation duration (*Sumich, 2001*; *Sumich & May, 2009*). While gray whale respiration rates in the field have been described during migration (*Sumich, 1983*) and foraging (*Wursig, Wells & Croll, 1986*; *Mallonee, 1991*; *Stelle, Megill & Kinzel, 2008*), these studies did not link respiration metrics to morphology or activity levels.

Gray whales are unique within baleen whales because they are suction feeders (*Nerini, 1984*). Within this species, Pacific Coast Feeding Group (PCFG) gray whales, which comprise a small (~212 individuals; *Harris et al., 2022*) subgroup of the Eastern North Pacific (ENP) population of gray whales (~19,260; *Eguchi, Lang & Weller, 2024*), feed in shallow, coastal habitats (<20 m depth; *Bird et al., 2024a*) between Northern California, USA, and Southern British Columbia, Canada (*Calambokidis, Perez & Laake, 2019*) during the summer months (June–November). PCFG gray whales use at least eight different foraging tactics (*Torres et al., 2018*; *Bird et al., 2024a*) to forage on a variety of benthic, epibenthic and pelagic invertebrates (*Darling, Keogh & Steeves, 1998*; *Dunham & Duffus, 2001*; *Hildebrand, Bernard & Torres, 2021*) in both rocky reef and sandy habitats (*Bird et al., 2024a*). These large capital-breeding baleen whales forage in a shallow niche despite having no obvious morphological adaptations for shallow diving (*e.g.*, unlike sirenians' dense bones, horizontal diaphragm and skeletal weight distribution; *Domning & de Buffrénil, 1991*). Despite this apparent lack of adaptation, PCFG gray whales persistently feed in this shallow niche and show high maternal recruitment (*Lang et al., 2014*; *Calambokidis & Pérez,*

2017), suggesting that this strategy is beneficial; however, a comprehensive assessment of their energetics during these shallow foraging dives is needed to better understand their ecology, physiology and response to disturbance.

There is individual variation in the use of foraging tactics across PCFG gray whales, and an ontogenetic shift in tactic use associated with growth in length (*Bird et al., 2024a*). Shorter, younger whales utilize forward moving behaviors and longer, older whales predominantly use stationary behaviors (*e.g.*, headstands; *Bird et al., 2024a*). Despite being one of the most prevalent tactics, headstanding appears to be costly. Fluke stroke rate, derived from accelerometry tags deployed on PCFG gray whales (*Colson et al., 2024*), indicates that headstanding is the most energetically costly foraging tactic relative to other tactics (*Colson, 2023*). However, PCFG gray whales appear to use bubble blasts, underwater releases of air that rises to surface and forms a circle/puka (*Torres et al., 2018*), as a behavioral adaptation during foraging dives to reduce the costs of buoyancy and extend dive times (*Bird et al., 2024b*). Combined, the links between body size, shifts in preferred foraging tactic, and bubble blast occurrence suggest that PCFG gray whales have developed behavioral adaptations to forage in this shallow niche, but energetic costs are variable by tactic, individual, and habitat type.

Drones and accelerometry tags can provide valuable respiration data, offering the potential to pair energy estimates with behavior. High-resolution, breath-by-breath metrics can be extracted from video footage (*Nazario et al., 2022*; *Sumich et al., 2023*), while breath counts and activity can be measured from tag data using accelerometry, depth, or acoustic data (*Fahlman et al., 2008b*; *Halsey et al., 2008*; *Roos, Wu & Miller, 2016*; *Isojunno et al., 2018*). Drones also provide concurrent individual morphology and body condition data (*Dawson et al., 2017*; *Torres et al., 2022*; *Bierlich et al., 2023*). Therefore, the high-resolution respiration data derived from these tools can advance our understanding of diving energetics in baleen whales (*Mysticeti*), for which physiological information is limited relative to other marine mammals (*Fahlman et al., 2016*). Furthermore, the shallow coastal habitat and site fidelity of PCFG gray whales provides an ideal system in which to study baleen whale energetics with high resolution data as individuals are accessible to be repeatedly sampled over time.

Here, we explore how morphology, body condition, and behavior affect PCFG gray whale respiration in a shallow foraging habitat. We aim to measure how energetic costs change with different dive characteristics and hypothesize that the energetic cost of a foraging dive increases with individual body length, body condition (associated with increased buoyancy) and dive duration and varies across different foraging tactics. Specifically, we use a unique seven-year longitudinal dataset of PCFG gray whale morphology, body condition, and behavior from drone footage and a two-year dataset of tag deployments to first examine metrics that could be used to test our hypothesis by (1) exploring a suite of respiration metrics that reflect PCFG gray whale energetics on their foraging grounds and (2) comparing respiration metrics derived from drone and tag data. We then test our hypothesis by (3) modeling how respiration metrics vary with body length, body condition, and behavior, (4) discerning whether respiration metrics indicate recovery from

or anticipation of a dive, and (5) simulating daily FMR using our results to contextualize energetic demands on a daily scale.

MATERIALS & METHODS

Data collection

We collected drone footage of PCFG gray whales filmed off the coast of Newport (44.60765, −124.08162) and Port Orford (42.737407, −124.505301), Oregon, United States, between June and October of 2016–2022 (Fig. 1). Drone operations were conducted in good weather conditions from a small (5.4 m) rigid hull inflatable boat (wind <22 km/h, swell <1.5 m, minimal fog or rain). *Ad libitum* (*Altmann, 1974*) boat-based surveys were conducted by teams of 3–4 people, and included photo-identification of individual whales.

Four different DJI drones were used over the course of this study: a Phantom 3 Pro, 4 Advanced and 4 Pro, and an Inspire 2. A laser altimeter (*e.g.*, "LidarBoX") was mounted on the Inspire 2 to provide more accurate photogrammetry measurements (*Dawson et al., 2017*; *Bierlich et al., 2024*). Details on the cameras mounted on each drone are available in supplementary (Table S2). The pilot recorded video continuously during flight (∼15 min) at an altitude between 20 and 40 m, during which the whale was located and followed while visible at the surface or underwater.

Throughout the 2021 and 2022 field seasons, nine suction-cup-attached Custom Animal Tracking Solution (CATS; https://cats.is) video and inertial measurement unit tags were deployed on nine individual whales using an 8 m carbon fiber pole from the boat (*Colson et al., 2024*). Tags were equipped with a gyroscope, 50 Hz magnetometer, 400 Hz accelerometer, 10 Hz pressure, temperature, light and GPS sensors, and a video camera and hydrophone. Each of the four suction cups on the tag had an oxidizing release to guarantee release after suction failed. All nine individuals tagged were also in the drone dataset.

Data was collected using drones and suction cup tags. Research was conducted under NOAA/ NMFS permits #16011 and #21678 and IACUC approval No.CRC-SOP-3. UAS operations were conducted by a Federal Aviation Authority (FAA) certified private pilot with a Part107 license. During field work, behaviour was observed for indications of a behavioural response to disturbance (changes in direction, increased swim speed, sudden dives) and none were observed. Disturbance potential was minimized by maintaining a slow boat speed when near whales and maintaining the drone at a minimum altitude of 20 m.

Data processing

Drone data

Video processing. Drone footage was first clipped to periods when a whale was visible, and the whale(s) in each clip were identified using an aerial catalog and photo-identification images taken during the flight. A single experienced analyst (CNB) then reviewed each clip at least twice per whale to annotate the behaviors performed using continuous focal sampling and the Behavioral Observation Research Interactive Software (BORIS; *Friard & Gamba, 2016*). We used an ethogram containing 49 behaviors (Table S1, *Torres et al., 2018*; *Bird et al., 2024a*). For this study we focused on forage and travel behaviors (Table 1). Foraging

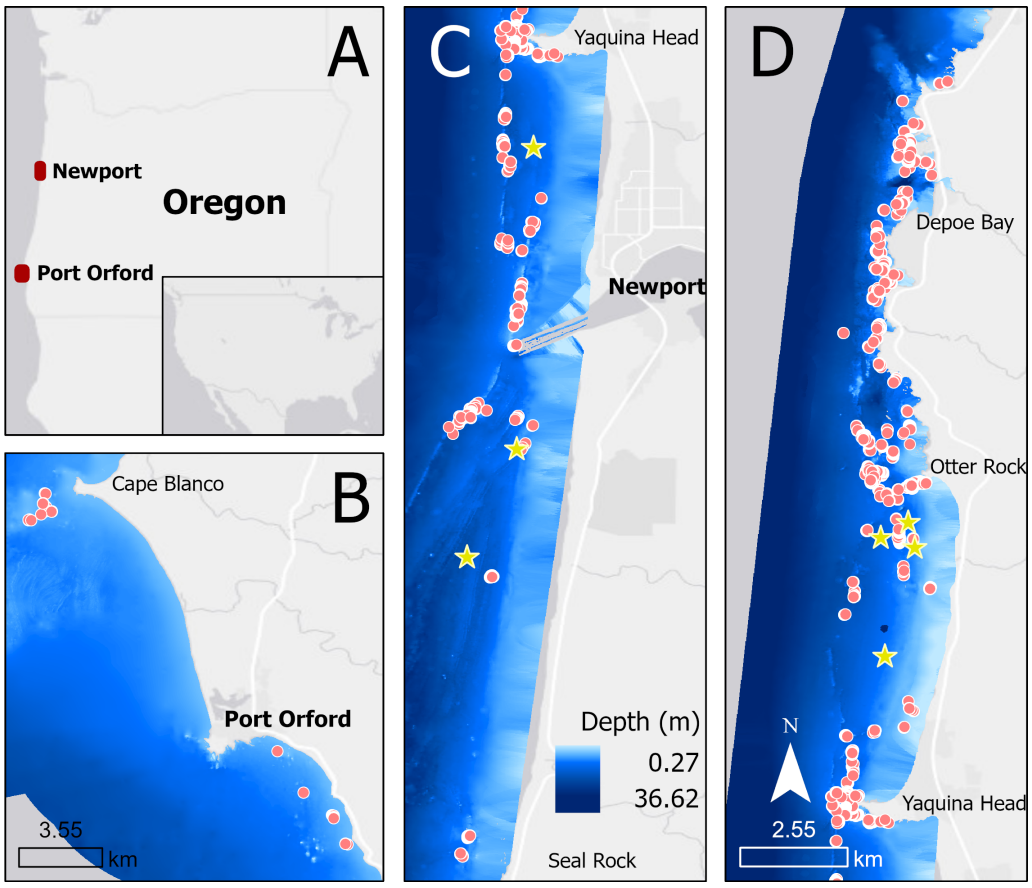

Figure 1 **Map showing locations of tag deployments (yellow stars) and drone observations (red dots) in Oregon (A), specifically off Port Orford (B) and Newport (split into C and D).**
Full-size DOI: 10.7717/peerj.20247/fig-1

behavior was defined down to the tactic level. Foraging tactics that were mechanically similar and tended to co-occur were grouped to increase sample size following *Bird et al. (2024a)* (Table 1). Therefore, all behaviors exhibited during a dive sequence were assignable to a single, mutually-exclusive category—except for bubble blasts, which could occur in coincidence with foraging tactics. Further filtering was applied to select only clips with at least one complete surfacing sequence in the footage, which was defined as sequences where the whale surfaced for the first time after a dive and started a new dive at the end of the sequence. Within each complete sequence, breaths were categorized as initial (the first breath in the sequence), terminal (the final breath in the sequence), or middle (any breath between the initial and terminal breaths). In single breath sequences, the breath was classified as initial.

Respiration metrics. We quantified the following respiration metrics from drone video review: surface sequence duration, individual breath inhalation duration, total inhalation duration, inter-breath interval (IBI), rate of inhalation accumulation, breath count, respiration rate, and nares area. Surface sequence duration was calculated as the number

Table 1 Ethogram containing definitions of PCFG gray whale behaviors included in this study. The complete ethogram is available in Table S1.

Primary behavior state	Tactic group	Sub-behavior tactics	Definition
Forage	Headstand	Headstand	Whale is positioned head down-flukes up, or if in water depths less than whale body length, whale may be more horizontal in water column; With both body positions the whale is observed pushing head/mouth region into substrate.
	Side-swim (stationary)	Side-swim (stationary)	Whale observed swimming on its side, but not moving forward. Characterized by frequent jaw snapping.
	Forward swimming tactics	Side-swim (forward)	Whale observed swimming on its side, moving forward. Characterized by frequent jaw snapping.
		Upside-down swim (forward)	Whale observed swimming upside-down, moving forward. Characterized by frequent jaw snapping.
		Subsurface (forward)	Whale swims subsurface while feeding. Characterized by frequent jaw snapping.
	Subsurface (stationary)	Subsurface (stationary)	Whale maintains a stationary position while feeding below the surface of the water, oriented dorsal up.
	Surface tactics	Surface feeding	Whale feeding at the surface, frequently breaking the surface but without breathing. Characterized by frequent turning and frequent jaw snapping/flexing.
		Skim feeding	Whale swims at the surface with mouth open for an extended period. Characterized by moving forward in a straight line.
	Bubble blast	Bubble blast	Underwater release of air by whale that rises to surface and forms a circle/puka.
Travel			Whale shows directed travel in a consistent direction, with regular surfacing intervals.

of seconds between the initial and terminal breaths. To calculate the inhalation duration of each breath, an analyst noted the start and end time of each breath (including exhalation immediately followed by an inhalation). The start was denoted as the time when bubbles started flowing out of the nares and the end as the moment the nares closed or became submerged underwater. Inhalation duration was calculated as one-half of the breath duration (*Sumich et al., 2023*). Total inhalation duration for a surface sequence was the sum of all the individual breath inhalation durations. IBI was the mean number of seconds between sequential breaths in a surface sequence (*Sumich, 1983*; *Stelle, Megill & Kinzel, 2008*). The rate of inhalation accumulation was calculated as the slope of the relationship between total inhalation duration and seconds since first breath, which represents a combination of inhalation duration and respiration rate and may reflect recovery strategy (*i.e.,* fast *versus* slow). One slope was calculated per surface sequence. The breath count was the total number of breaths observed in the surface sequence. Respiration rate (breaths min^{-1}) was calculated for travelling whales as the total breath count for the observation period divided by the total travel duration for that whale (*Sumich, 1983*; *Spina et al., 2024*).

To explore the relationship between nares area and oxygen exchange we measured the maximum nares area (m^2) during an inhalation. To measure maximum area, a snapshot was extracted at the midpoint of the inhalation when the flow rate was highest (*Sumich & May, 2009*). Snapshots were then filtered for quality; only clear images where the nares were

not obstructed by the blow were retained (Fig. S1, Table S3). Nares were measured using MorphoMetriX (*Torres & Bierlich, 2020*) and processed using CollatriX (*Bird & Bierlich, 2020*). The length and width were measured using the 'Measure Length' function and area was measured using 'Measure Area' (Fig. S2). In a subset of 30 randomly selected snapshots, both the left and right nares were measured to test the assumption that they were equal. In all remaining images, only the clearest naris was measured. For comparisons across individuals, the area was standardized by the individuals' total length (TL). This metric was only measured on a subset of the data (2020–2021; $n = 183$ breaths).

Individual length and body condition. The total length (TL) and body area index (BAI) of each individual in this study was estimated from snapshots extracted from drone footage following photogrammetry methods described in *Torres et al. (2022)*. Measurements were made manually using MorphoMetriX (*Torres & Bierlich, 2020*) and processed using CollatriX (*Bird & Bierlich, 2020*). A posterior predictive distribution for TL was generated using a Bayesian statistical model to account for photogrammetric uncertainty and growth (*Bierlich et al., 2021b*; *Pirotta et al., 2024*). One TL per individual per year was estimated, as individuals were not expected to significantly grow during a foraging season. BAI, a standardized measure of body condition that changes more rapidly than TL (*Burnett et al., 2018*; *Bierlich et al., 2021a*), was calculated on the same day for which behaviors were scored. If there were no BAI measurements from the date of the behavior observation, the nearest measurement within ±14 days was selected (*Pirotta et al., 2023*).

Travel swim speed. Swim speed during travel was derived from the drone's GPS (*Christiansen et al., 2023*). Speed was only calculated for periods when the drone was directly over the whale. GPS position was extracted every 5 s and the distance between the points was divided by time to calculate speed in m s^{-1}. Speed was then averaged across the entire observation period.

Tag data

We used data from nine tag deployments on nine individual whales. The mean deployment duration was 9.14 hr (range = 0.44 h to 24.81 hr; *Colson et al., 2024*).

Behavior. We used the primary behavior state (forage, search, and travel) and foraging tactic (headstand, side swim, and benthic dig) event classifications from *Colson et al. (2024)*. *Colson et al. (2024)* assigned primary behavior states based on turn angle, dive duration, pseudotrack tortuosity, and roll presence using hidden Markov models, while foraging tactics were classified by median pitch, absolute median roll, and the depth to TL ratio using a classification and regression tree (CART) model (with 84.8% accuracy). Consecutive travel dives were grouped into a travel series.

Breath count. Surface sequences between dives were identified during manual examination of the tag deployment's depth profile (*Colson et al., 2024*). Breaths during a surface sequence were identified as surfacings that occurred between very shallow dives identified using the 'find_dives' function from the package *tagtools* (*DeRuiter et al., 2024*) with a minimum

depth of 0.2 m. To validate our methods, we compared breath timestamps identified from tag and drone data during a single six-minute clip when the drone was over a tagged whale; this validation confirmed that the surfacings between shallow dives aligned with breaths in the drone footage. We also determined that, in the tag data, any surfacing longer than 10 s represented at least two breaths. Thus, we counted every surfacing longer than 10 s as two breaths. This breath count metric represents a minimum estimate, given that breaths could be missed. Respiration rate was calculated for traveling whales as the minimum breath count divided by the total travel series time.

Statistical analysis

Analyses were performed in R v4.4.2 (*R Core Team, 2024*). Bayesian models used *RStan* (*Stan Development Team, 2020*), and *rethinking* (*McElreath, 2020*). All data and code are available at: https://doi.org/10.6084/m9.figshare.26999995.v1.

Metric exploration

Nares area. Frequentist linear models were used to assess the relationships between the right and left nares (fitting separate models for length, width, and area), and the relationships between TL and the mean nares length, width, and area. Finally, a linear mixed effect model (LMM) was used to assess how nares area, standardized by TL, varied across breath types (initial, middle, terminal), accounting for individual ID as a random effect. Nakagawa's R^2 was used to assess the goodness-of-fit of the LMMs (*Nakagawa & Schielzeth, 2013*).

Correlation of metrics. Prior to model development, all respiration metrics from the drone data were summarized at the surface sequence scale. Pearson correlation coefficients were used to explore linear correlations between the respiration metrics.

Respiration models. Several models were run to investigate how each respiration metric varied as a function of body length, body condition, and behavior (Table 2). We ran separate foraging and travelling models; in the foraging models behavior included bubble blast occurrence, dive duration, and tactic, and in the travelling models behavior was only swim speed. To incorporate uncertainty in the measurement of TL and BAI, their values were imputed within the Bayesian model from their posterior distributions. TL, BAI, mean swim speed, and dive duration were z-score standardized and used as fixed effects. Continuous respiration metrics were log-transformed to meet model assumptions. All models were fit in a Bayesian framework as it allows for the incorporation of photogrammetric uncertainty associated with drone-based measurements. Prior distributions for all model parameters are given in Tables S8, S10, S11, S14 of the supplementary. For all models, we assessed convergence using effective sample size, $\hat{R}$ values, and visual examination of trace plots (*McElreath, 2020*). Visual examination of the residuals, bayes R^2 (*Gelman et al., 2019*), and posterior predictive checks were used to assess model fit. Model coefficients were interpreted using the posterior 95% credible intervals and their percent overlap with zero.

Table 2 **All models and metrics.**

Hypothesis	Response[a]	Fixed effects[b]	Timing	Random effect	Error structure
Foraging: Recovery	Breath count (drone)	TL, BAI, dive duration, bubble blast occurrence, foraging tactic	Bubble blast occurrence, dive duration, and foraging tactic from the dive following the surface sequence	Individual ID	Poisson (log link)
	Breath count (tag)	TL, BAI, dive duration, foraging tactic		Individual ID	Poisson (log link)
	Total inhalation duration	TL, BAI, dive duration, bubble blast occurrence, foraging tactic		Individual ID	Gaussian (log transformed response)
	Mean inter-breath interval (IBI)	TL, BAI, dive duration, bubble blast occurrence, foraging tactic		Individual ID	Gaussian (log transformed response)
	Rate of inhalation accumulation	TL, BAI, dive duration, bubble blast occurrence, foraging tactic		Individual ID	Gaussian (log transformed response)
	Intial breath inhalation duration	TL, BAI, dive duration, bubble blast occurrence, foraging tactic		Individual ID	Gaussian (log transformed response)
Foraging: anticipation	Total Inhalation Duration	TL, BAI, dive duration, bubble blast occurrence, foraging tactic	Bubble blast occurrence, dive duration, and foraging tactic from the dive following the surface sequence	Individual ID	Gaussian (log transformed response)
	Mean inter-breath interval (IBI)	TL, BAI, dive duration, bubble blast occurrence, foraging tactic		Individual ID	Gaussian (log transformed response)
	Rate of inhalation accumulation	TL, BAI, dive duration, bubble blast occurrence, foraging tactic		Individual ID	Gaussian (log transformed response)
	Terminal breath inhalation duration	TL, BAI, dive duration, bubble blast occurrence, foraging tactic		Individual ID	Gaussian (log transformed response)
Foraging: recovery and anticipation	Total Inhalation Duration	TL, BAI, dive duration, foraging tactic	Dataset was filtered to only surface sequences where the same foraging tactic was used in both the preceding and following dive	Individual ID	Gaussian (log transformed response)
	Mean inter-breath interval (IBI)	TL, BAI, dive duration, foraging tactic		Individual ID	Gaussian (log transformed response)
	Rate of inhalation accumulation	TL, BAI, dive duration, foraging tactic		Individual ID	Gaussian (log transformed response)
Travel	Respiration rate	TL, BAI, travel swim speed		Individual ID	Gaussian (log transformed response)

Notes.

[a]All response metrics were log transformed.

[b]All fixed effects were scaled.

Foraging models. We checked for autocorrelation in model residuals using Poisson log-linear models for breath count. We selected this respiration metric as it was available from both drones and tags and was highly correlated with total inhalation duration (Fig. S6). The model for breath counts from the drone data included TL, BAI, preceding dive duration, bubble blast occurrence, and foraging tactic as fixed effects. The model for breath counts from the tag data included the same fixed effects except for bubble blast occurrence, which was unavailable from the tag data.

LMMs were used to assess how the natural log of total inhalation duration, IBI, the rate of inhalation accumulation, breath count, and the initial or terminal breath inhalation durations varied with TL, BAI, and behavior. We ran models to test the hypotheses that respiration is informative of a whale's recovery from a dive, their anticipation of the next dive, or some combination of both. The recovery models used the bubble blast occurrence, dive duration, and foraging tactic from the dive preceding the surface sequence. The anticipation models used behaviors from the dive following the surface sequence. The combined model used only surface sequences where the preceding and following foraging tactics were the same, did not include bubble blast occurrence as a fixed effect, and included both the preceding and following dive durations as fixed effects. TL and BAI were included in all models along with an individual-level random effect. The other explanatory variables differed amongst the model sets depending on data availability (see Table 2). This approach gave a total of 12 models, each of which was run for three chains of 90,000 iterations with the first 30,000 as warm-up.

Travel model. We used an LMM to evaluate the relationship of respiration rate during travel (derived from the drone data) with TL, BAI, and mean swim speed, including individual ID as a random effect. We ran three chains of 30,000 iterations with 10,000 as warm-up.

FMR and prey requirement simulation

To contextualize model results within gray whale energetics, we used Monte Carlo simulations to estimate field metabolic rate (FMR) in megajoules (MJ) at a daily scale using respiration metric values predicted from the models described above. For the simulations, we investigated the effects of TL, BAI, dive duration, and behavior on FMR. We simulated two TL values (9 and 12 m), three BAI values (22, 27, 32), three dive durations (60, 120, 300 s), and two foraging tactics (headstanding and forward swimming), thus capturing the range of explanatory variables evaluated for PCFG whales. These values resulted in 36 unique combinations of covariates for which FMR was simulated. Before running the simulations, we used the recovery models to predict total inhalation duration, breath count, and IBI for each of the 36 unique covariate combinations.

Daily FMR was calculated following the methods described in *Villegas-Amtmann et al. (2015)*:

$$FMR_{daily} = H \cdot \%O_2 \cdot V_{T(daily)}. \quad (1)$$

For heat production, H (MJ L^{-1} O_2 consumed), we used a value of 0.002 from *Kleiber (1961)*. For O_2 extraction efficiency, $\%O_2$, we drew a value from a normal distribution

at each iteration, using the mean (11%) and standard deviation (2.7%) calculated by *Villegas-Amtmann et al. (2015)* using data from *Sumich (2001)*. We estimated tidal volume (V_T) following Eq. (2) (*Sumich et al., 2023*), where tidal volume is estimated using the inhalation (or exhalation) duration (t_{in}) of a breath multiplied by the square of TL. While most studies multiply the tidal volume for a single breath by an estimated respiration rate to calculate FMR, we calculated a total daily tidal volume by multiplying the square of TL by the sum of the total inhalation durations within a day, $t_{in(daily)}$. As a result, daily tidal volume was:

$$V_{T(daily)} = -7.24 + 2.14 \cdot t_{in(daily)} \cdot TL^2. \quad (2)$$

To calculate the sum of the total inhalation durations within a day, we first divided the day into foraging hours and travel/search hours using the activity budget from *Colson et al. (2024)* (36% of time foraging, 43% of time searching, and 21% of time traveling). For the purposes of this simulation, travel and search were combined as their stroke rates are not significantly different (*Colson, 2023*).

For each of the 36 covariate combinations, we simulated complete dive and recovery cycles during foraging periods. We began by drawing a value for the breath count from the corresponding posterior distribution from the recovery models. This value was used as the mean of a Poisson distribution to generate a simulated breath count for each surface sequence. The simulated breath count determined the number of IBIs that followed a dive, and the length of these intervals was drawn from the posterior distribution of IBI from the recovery models. Total inhalation duration was also drawn from the corresponding posterior distribution. Together, the simulated dive duration, summed IBIs, and total inhalation duration represented a complete dive and recovery cycle. We simulated complete dive and recovery cycles for the foraging period until the total time spent in this activity state was equal to the expected number of hours in a 24-hour period. The same process was carried out for the travel/search hours; however, we resampled breath hold and inhalation durations from distributions with mean and standard deviation derived from the entire travel dataset, as our travel models showed no notable relationships between respiration rate and TL, BAI, or speed (see 'Results' section). Within the travel/search period, we iteratively drew a breath hold duration from a lognormal distribution of breath holds (log mean: 3.66, s.d: 0.65) and an inhalation duration from a lognormal distribution of inhalation durations (log mean: 0.26, s.d: 0.17). The two values were then added, and the process was repeated until the sum reached the total travel/search time for the day.

The total inhalation durations from both foraging and travel/search hours were summed to obtain $t_{in(daily)}$. Total daily tidal volume (Eq. (2)) was then used to calculate daily FMR (Eq. (1)). Finally, within each simulation, we estimated prey requirements to sustain daily FMR using the caloric value for composite PCFG prey (1.91 kJ g^{-1}), assuming equal proportions of the three main prey types in the region: *Holmesimysis sculpta*, *Neomysis rayii*, and *Atylus tridens* (*Hildebrand, Bernard & Torres, 2021*). A total of 20,000 Monte Carlo iterations were run per combination of covariates, and Cohen's *d* (mean, s.d) was used to compare FMR estimates across simulations (*Cohen, 1988*). We summarized Cohen's *d* values across covariate comparisons (TL, BAI, dive duration) where all other covariates

were constant (*e.g.*, we summarized Cohen's *d* across the multiple combinations where only the TL was different).

RESULTS

Metric exploration

Nares area

Our nares area dataset included 183 breaths from 21 individual whales across 70 surface sequences. Seventeen individuals were observed in only one year, and four were observed in two years. There were strong relationships between the left and right measurements for nares area (slope = 0.89, Confidence Interval $(CI)_{95}$ [0.72–1.06], R^2: 0.81, $F_{(1,27)}$: 116.16, p: 2.78×10^{-11}), length (slope = 0.81, CI_{95} [0.63–1.00], R^2: 0.76, $F_{(1,27)}$: 84.42, p: 8.46×10^{-10}), and width (slope = 0.70, CI_{95} [0.56–0.84], R^2: 0.79, $F_{(1,27)}$: 100.07, p: 8.46×10^{-10}) (Fig. S3). There were positive relationships between TL and mean nares area (slope = 0.0003, CI_{95} [0.0002–0.0004], R^2: 0.55, $F_{(1,19)}$: 23.64, p: 0.0001), length (slope = 0.01, ($CI_{95:}$ [0.01–0.02]), R^2: 0.46, $F_{(1,19)}$: 17.23, p: 0.0005), and width (slope = 0.01, ($CI_{95:}$ [0–0.01]), R^2: 0.36, $F_{(1,19)}$: 10.52, p: 0.004) (Fig. S4). The LMM comparing standardized nares area by behavior states and breath types while accounting for individual ID found no significant contrasts and had a conditional R^2 of 0.42 and a marginal R^2 of 0.01 indicating that there were no notable differences between breath types (initial, middle, terminal) for either absolute nares area (m^2) or length standardized nares area (Fig. S5).

Correlation of metrics

After filtering clips, we had 557 surface sequences from 88 unique individual whales. However, not all sequences had both a preceding dive and a following dive available, and some respiration metrics had more missing values than others, resulting in different sample sizes per metric (Table S7). Summaries of the metrics are available in the supplementary (Table S6). Of the metrics, total inhalation duration and breath count were the most correlated (0.96), while the others had Pearson correlation coefficients below 0.6 (Fig. S6).

Respiration models

Foraging

For all models, assessment of the residual plots indicated that model assumptions were met, and prior sensitivity analysis indicated no influence of prior choice. Bayes R^2 values are reported in Tables 3 and 4. Results of the posterior predictive checks are available in Tables S9, S12, S13, S16.

Recovery

Breath count from both drone and tag data. The results from the drone and tag data models were in agreement: TL, BAI, and preceding dive duration had a positive relationship with breath count (Fig. 2, Table 3). In the tag model, the side-swim forward tactic had a detectably higher breath count than headstanding (coefficient: 0.166, Credible Interval (CrI_{95}): 0.012, 0.319). There was no identifiable difference between tactics in the drone model, although subsurface stationary and the surface tactics did have the lowest predicted

Table 3 **Recovery model results.** Posterior mean and 95% credible intervals for each coefficient and the percentage of the posterior distribution that is above or below 0. Coefficients with at least 95% of the posterior distribution over (+/-) zero are bolded.

	Breath count (drone)		Breath count (tag)		Total inhalation duration		Inter-breath interval (IBI)		Inhalation accumulation rate		Initial breath duration	
Fixed effect	**mean (95% CrI)**	**% over (+/-) 0**	**mean (95% CrI)**	**% over (+/-) 0**	**mean (95% CrI)**	**% over (+/-) 0**	**mean (95% CrI)**	**% over (+/-) 0**	**mean (95% CrI)**	**% over (+/-) 0**	**mean (95% CrI)**	**% over (+/-) 0**
Intercept	0.83 (0.69, 0.96)	100	1.05 (0.68, 1.36)	100	1.01 (0.89, 1.13)	100	2.64 (2.52, 2.76)	100	−2.24 (−2.39, −2.1)	100	0.35 (0.3, 0.39)	100
Total length (TL)	0.07 (−0.03, 0.18)	91	0.08 (−0.12, 0.29)	82	**0.08 (−0.01, 0.17)**	**96**	**0.21 (0.11, 0.3)**	**100**	**−0.19 (−0.3, −0.08)**	**100**	0.02 (−0.02, 0.06)	85
Body area index (BAI)	**0.11 (0.01, 0.2)**	**99**	0.14 (−0.15, 0.42)	87	**0.08 (0, 0.16)**	**97**	**−0.07 (−0.15, 0.01)**	**96**	**0.09 (0, 0.19)**	**98**	−0.01 (−0.04, 0.01)	88
Bubble blast	−0.02 (−0.27, 0.23)	55	–	–	0.02 (−0.22, 0.27)	57	0.09 (−0.11, 0.29)	82	−0.08 (−0.33, 0.17)	73	−0.03 (−0.08, 0.03)	84
Dive duration	**0.16 (0.07, 0.23)**	**100**	**0.2 (0.15, 0.24)**	**100**	**0.16 (0.08, 0.24)**	**100**	**−0.13 (−0.2, −0.05)**	**100**	**0.13 (0.04, 0.22)**	**100**	0.01 (−0.01, 0.03)	79
Forward swimming	−0.15 (−0.39, 0.08)	90	–	–	−0.09 (−0.28, 0.11)	81	**0.19 (0, 0.37)**	**97**	**−0.28 (−0.5, −0.07)**	**99**	−0.03 (−0.08, 0.03)	83
Subsurface stationary	**−0.39 (−0.89, 0.07)**	**95**	–	–	**−0.38 (−0.76, 0.01)**	**97**	**−0.12 (−0.52, 0.29)**	72	−0.21 (−0.73, 0.31)	79	**−0.09 (−0.18, 0.01)**	**97**
Side-swim stationary	−0.02 (−0.34, 0.29)	54	–	–	−0.14 (−0.41, 0.12)	86	−0.14 (−0.42, 0.15)	83	−0.02 (−0.38, 0.34)	54	−0.04 (−0.1, 0.03)	88
Surface tactics	**−0.44 (−0.86, −0.05)**	**99**	–	–	**−0.51 (−0.83, −0.19)**	**100**	−0.09 (−0.49, 0.3)	67	−0.35 (−0.88, 0.19)	90	**−0.12 (−0.24, −0.01)**	**98**
Side-swim fwd	–	–	**0.17 (0.01, 0.32)**	**98**	–	–	–	–	–	–	–	–
Benthic dig	–	–	0 (−0.12, 0.12)	52	–	–	–	–	–	–	–	–
Individual random effect	0.08 (0.01, 0.21)	100	0.39 (0.17, 0.87)	100	0.09 (0.01, 0.22)	100	0.22 (0.09, 0.34)	100	0.2 (0.05, 0.35)	100	0.13 (0.1, 0.17)	100
Bayes R^2	0.41 (0.35, 0.46)	–	0.33 (0.30, 0.36)	–	0.26 (0.17, 0.34)	–	0.49 (0.35, 0.59)	–	0.46 (0.34, 0.57)	–	0.59 (0.52, 0.65)	–

Table 4 Anticipation model results. Posterior mean and 95% credible intervals for each coefficient and the percentage of the posterior distribution that is above or below 0. Coefficients with at least 95% of the posterior distribution over (+/-) zero are bolded.

	Total inhalation duration		Inter-breath interval (IBI)		Inhalation accumulation rate		Terminal breath duration	
Fixed effect	**mean (95% CrI)**	**% over (+/-) 0**	**mean (95% CrI)**	**% over (+/-) 0**	**mean (95% CrI)**	**% over (+/-) 0**	**mean (95% CrI)**	**% over (+/-) 0**
Intercept	0.86 (0.72, 0.99)	100	2.59 (2.44, 2.74)	100	−2.21 (−2.4, −2.02)	100	0.34 (0.28, 0.41)	100
Total length (TL)	0.04 (−0.06, 0.14)	78	**0.21 (0.09, 0.32)**	**100**	**−0.2 (−0.33, −0.06)**	**100**	−0.01 (−0.07, 0.04)	65
Body area index (BAI)	0.05 (−0.04, 0.15)	87	**−0.11 (−0.21, −0.01)**	**99**	**0.18 (0.05, 0.31)**	**100**	0.02 (−0.01, 0.05)	91
Bubble blast	0.19 (−0.08, 0.46)	92	−0.01 (−0.26, 0.23)	54	−0.03 (−0.36, 0.31)	57	−0.01 (−0.08, 0.06)	60
Dive duration	−0.01 (−0.1, 0.08)	61	0.01 (−0.08, 0.1)	58	−0.03 (−0.15, 0.09)	70	0 (−0.03, 0.02)	57
Forward swimming	−0.07 (−0.28, 0.14)	74	**0.25 (0.03, 0.47)**	**99**	**−0.37 (−0.65, −0.1)**	**100**	−0.04 (−0.11, 0.03)	88
Subsurface stationary	**−0.41 (−0.83, 0)**	**97**	**1.19 (0.36, 2.02)**	**100**	**−1.42 (−2.32, −0.5)**	**100**	0.07 (−0.11, 0.24)	77
Side-swim stationary	0.04 (−0.28, 0.35)	60	0.05 (−0.26, 0.35)	62	−0.17 (−0.56, 0.22)	81	**−0.09 (−0.18, 0)**	**98**
Surface tactics	**−0.48 (−0.82, −0.13)**	**100**	0.08 (−0.42, 0.58)	62	−0.44 (−1.08, 0.21)	91	0.17 (−0.06, 0.4)	92
Individual random effect	0.1 (0.01, 0.25)	100	0.23 (0.09, 0.37)	100	0.22 (0.03, 0.42)	100	0.17 (0.12, 0.22)	100
Bayes R^2	0.16 (0.08, 0.26)	–	0.46 (0.30, 0.59)	–	0.48 (0.35, 0.60)	–	0.69 (0.61, 0.75)	–

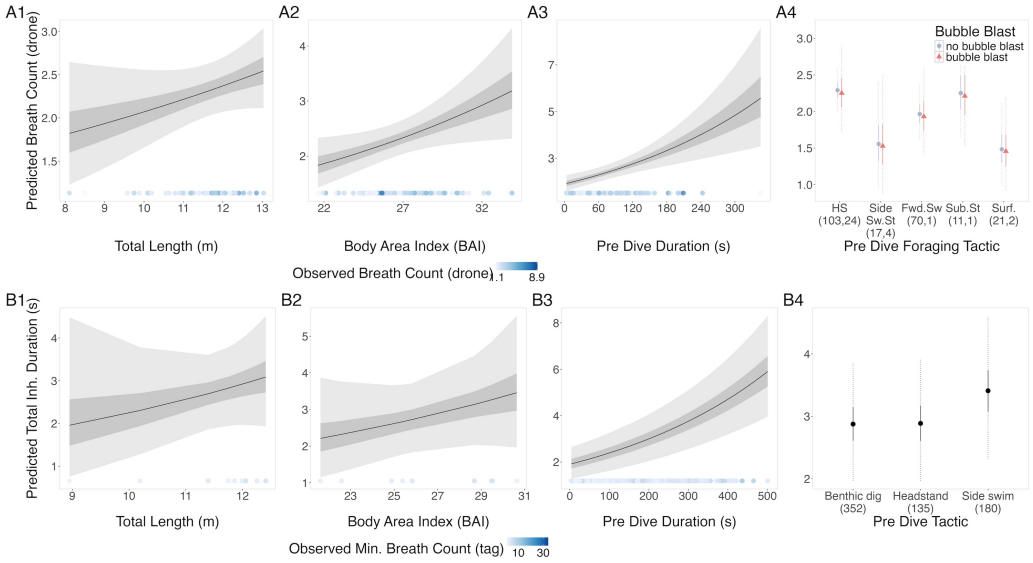

Figure 2 Estimated relationships between breath count per sequence from (A) drone data and (B) tag data. Relationships between breath count per sequence and (1) total length (TL), (2) Body Area Index (BAI), (3) preceding dive duration (s) and (4) preceding dive foraging tactic and bubble blast occurrence (in A only). The response variable was transformed from the log scale back to breath counts. In columns 1, 2, and 3, the line represents the mean posterior relationship, the dark gray shaded region represents the 50% credible interval, and the light gray shaded region represents the 95% credible interval. The points along the *x*-axis in each plot represents the original data values, colored by the observed breath count with darker shades representing higher values. In column 4, the points represent the posterior mean breath counts, the solid lines represent the 50% credible intervals, and the dashed lines represent the 95% credible intervals. In A4 the tactics are abbreviated as follows: HS, Headstand; Side.Sw.St, Side-swim stationary; Fwd.Sw., Forward swimming tactics; Sub.St, Subsurface stationary; Surf., Surface tactics; grey circles indicate that no bubble blast occurred, while orange triangles indicated the occurrence of a bubble blast. The sample sizes per tactic are reported in parentheses under the tactic name: the first value indicates the number of observations with no bubble blast for that tactic, and the second value indicates the number of observations with a bubble blast for that tactic.

Full-size DOI: 10.7717/peerj.20247/fig-2

breath counts. Autocorrelation was not an issue in the residuals of either model. The dispersion parameter of the drone and tag models were 0.68 and 1.7, respectively.

Total inhalation duration. TL, BAI, and preceding dive duration all had a positive relationship with total inhalation duration, while bubble blast occurrence had no notable relationship (Figs. 3A1–3A4, Table 3). Side swimming stationary and the surface tactics had the shortest log-transformed total inhalation durations, specifically the surface tactics were associated with notably shorter durations compared to headstanding and the forward swimming tactics.

Inter-breath interval (IBI). TL had a positive relationship with mean IBI, while BAI and preceding dive duration had a negative relationship, and bubble blast occurrence had no notable relationship (Figs. 3B1–3B4, Table 3). Forward swimming was associated with the longest IBI, which was notably longer than that of side-swimming stationary.

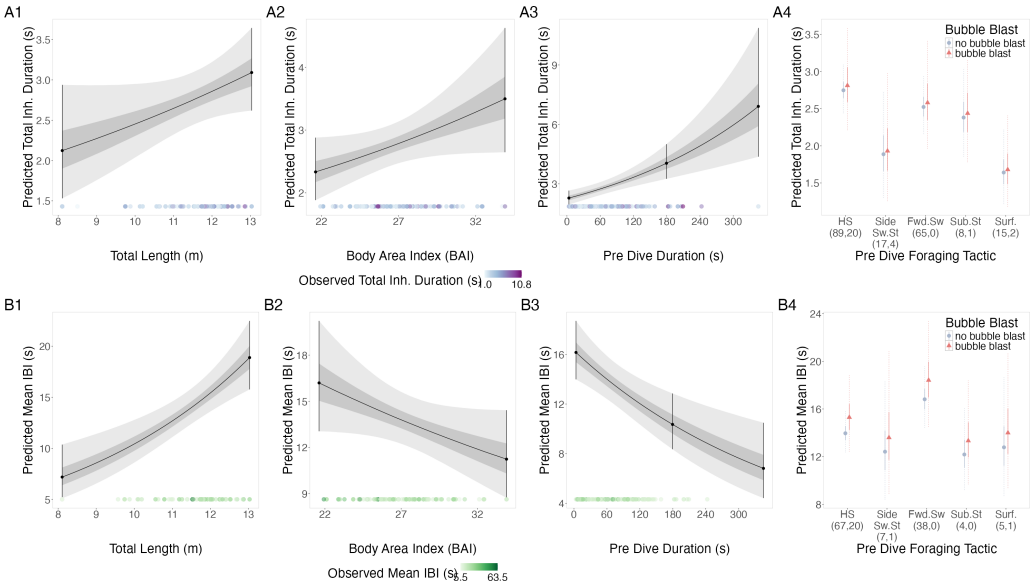

Figure 3 Estimated relationships from the "recovery models". Relationships between (1) total length (TL), (2) body area index (BAI), (3) preceding dive duration (s) and (4) preceding dive foraging tactic and bubble blast occurrence and (A) total inhalation duration (s) and (B) mean inter-breath interval (IBI). All response variables were transformed from the log scale to seconds. In columns 1, 2, and 3, the line represents the mean posterior relationship, the dark gray shaded region represents the 50% credible interval, and the light gray shaded region represents the 95% credible interval. Points with bars represent the mean probability and 95% credible interval at the minimum and maximum (1) TL and (2) BAI. In (3) preceding dive duration, points with bars represent the mean value and 95% credible interval at the minimum and maximum dive duration and 3- minute dive durations. The points along the *x*-axis in each plot represents the original data values, colored by the observed values of each row's respective response variable with darker shades representing higher values. In column 4, the points represent the posterior mean values, the solid lines represent the 50% credible intervals, and the dashed lines represent the 95% credible intervals. In column 4 the tactics have been abbreviated as follows: HS, Headstand; Side.Sw.St, Side-swim stationary; Fwd.Sw., Forward swimming tactics; Sub.St, Subsurface stationary; Surf., Surface tactics. Grey circles indicate that no bubble blast occurred, while orange triangles indicated the occurrence of a bubble blast. The sample sizes per tactic are reported in parentheses under the tactic name: the first value indicates the number of observations with no bubble blast for that tactic, and the second value indicates the number of observations with a bubble blast for that tactic. Note that the *Y*-axis scale is free; a fixed-scale version is available in Fig. S7.

Full-size DOI: 10.7717/peerj.20247/fig-3

Inhalation accumulation rate. TL had a negative relationship with the log-transformed inhalation accumulation rate, while BAI and preceding dive duration had a positive relationship. There was no association with bubble blast occurrence (Figs. S8A1–S8A4, Table 3). Inhalation accumulation rate was greatest after headstanding and subsurface stationary; with no overlap between the credible intervals for headstanding and the forward swimming tactics.

Initial breath inhalation duration. TL, BAI, preceding dive duration, and bubble blast occurrence did not have a detectable relationship with the log-transformed inhalation duration of the initial breath in a sequence (Figs. S8B1–S8B4, Table 3). Generally, side

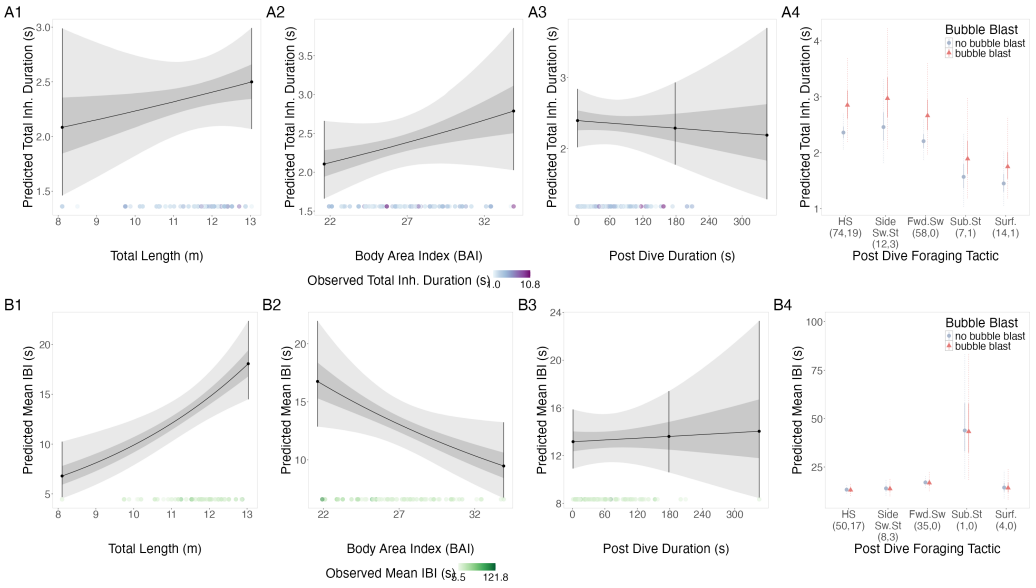

Figure 4 Estimated relationships from the "anticipation models". Relationships between (1) total length (TL), (2) Body Area Index (BAI), (3) following dive duration (s) and (4) following dive foraging tactic and bubble blast occurrence on (A) total inhalation duration (s) and (B) mean inter-breath interval (IBI). All response variables were transformed from the log scale to seconds. In columns 1, 2, and 3, the line represents the mean posterior relationship, the dark gray shaded region represents the 50% credible interval, and the light gray shaded region represents the 95% credible interval. Points with bars represent the mean value and 95% credible interval at the minimum and maximum (1) TL and (2) BAI. In (3) preceding dive duration, points with bars represent the mean value and 95% credible interval at the minimum and maximum dive duration and 3- minute dive durations. The points along the *x*-axis in each plot represents the original data values, colored by the observed values of each row's respective response variable with darker shades representing higher values. In column 4, the points represent the posterior mean values, the solid lines represent the 50% credible intervals, and the dashed lines represent the 95% credible intervals. In column 4 the tactics have been abbreviated as follows: HS, Headstand; Side.Sw.St, Side-swim stationary; Fwd.Sw., Forward swimming tactics; Sub.St, Subsurface stationary; Surf., Surface tactics. Grey circles indicate that no bubble blast occurred, while orange triangles indicated the occurrence of a bubble blast. The sample sizes per tactic are reported in parentheses under the tactic name: the first value indicates the number of observations with no bubble blast for that tactic, and the second value indicates the number of observations with a bubble blast for that tactic. Note that the *Y*-axis scale is free; a fixed-scale version is available in Fig. S8.

Full-size DOI: 10.7717/peerj.20247/fig-4

swim stationary and the surface tactics had the lowest inhalation durations, with that of the surface tactics being notably lower compared to headstanding.

Anticipation

Total inhalation duration. There were no notable relationships of the log-transformed total inhalation duration with TL, BAI, following dive duration, or bubble blast occurrence (Figs. 4A1–4A4, Table 4). However, the surface tactics were associated with a notably lower log total inhalation duration compared to other tactics.

Inter-breath interval (IBI). TL had a positive relationship with log-transformed IBI, BAI had a negative relationship, while following dive duration and bubble blast occurrence

showed no relationship (Figs. 4B1–4B4, Table 4). Subsurface stationary and the forward swimming tactics were associated with the longest log IBIs.

Inhalation accumulation rate. Log-transformed inhalation accumulation rate had a negative relationship with TL and a positive relationship with BAI (Figs. S10A1–S10A4, Table 4). Subsurface stationary and the forward swimming tactics were both associated with low log rates compared to the other tactics.

Terminal breath inhalation duration. TL, BAI, following dive duration, and bubble blast occurrence did not have detectable relationships with the log-transformed terminal breath inhalation duration (Figs. S10A1–S10A4, Table 4). Side-swim stationary was associated with the lowest log terminal inhalation duration. The posterior distribution of the random effect did not overlap with 0 for 12 of the 44 individuals.

Recovery and anticipation model

Preceding dive duration had a positive relationship with log-transformed total inhalation duration (coefficient: 0.182, CrI_{95}: 0.081, 0.283), while TL, BAI, and the following dive duration did not (Table S14), as suggested by the overlap of the posterior credible intervals with 0. Assessment of the residual plots indicated that model assumptions were met. The Bayes R^2 was 0.342 (CrI_{95}: 0.225, 0.440).

Travel models

TL, BAI, and swim speed did not show a notable relationship with log-transformed respiration rate during travel, as suggested by the overlap of their 95% CrI with 0 (Fig. S11, Table S17). Specifically, there was an 84% estimated probability that respiration rate during travel increased with TL (coefficient: 0.115, CrI_{95}: −0.116, 0.342). BAI had a 78% estimated probability of a positive relationship (coefficient: 0.084, CrI_{95}: −0.131, 0.298), while there was a 73% probability of a negative relationship with swim speed (coefficient: −0.060, CrI_{95}: −0.259, 0.139). Assessment of the residual plots indicated that model assumptions were met, and the Bayes R^2 value was 0.355 (CrI_{95}: 0.057, 0.658).

FMR and prey requirement simulations

Daily FMR increased with TL and BAI, decreased with dive duration, and was marginally higher for headstanding than the forward swimming tactics (Fig. 5, Table 5). The highest simulated daily FMR was for a 12-m whale with a BAI of 32 that only foraged using 60-second headstanding dives (FMR: 1,725.24 MJ day^{-1}, CI_{95}: 914.06, 2,585.37), resulting in an estimated daily prey requirement of 0.85 metric tons (CI_{95}: 0.45, 1.28). The lowest simulated daily FMR was for a 9-m whale with a BAI of 22 that only foraged using 300-second forward swimming dives (FMR: 719.81 MJ day^{-1}, CI_{95}: 383.49, 1,071.52), requiring an estimated 0.36 (CI_{95}: 0.19, 0.53) metric tons of prey per day. Controlling for all other variables, the difference in FMR given a 12- *versus* a 9-m TL had the largest Cohen's *d* (mean: 2.26, s.d: 0.07), corresponding to differences in FMR and prey requirements of 669.51 MJ day^{-1} (s.d: 37.14) and 0.35 metric tons (s.d: 0.02), respectively (Table 5).

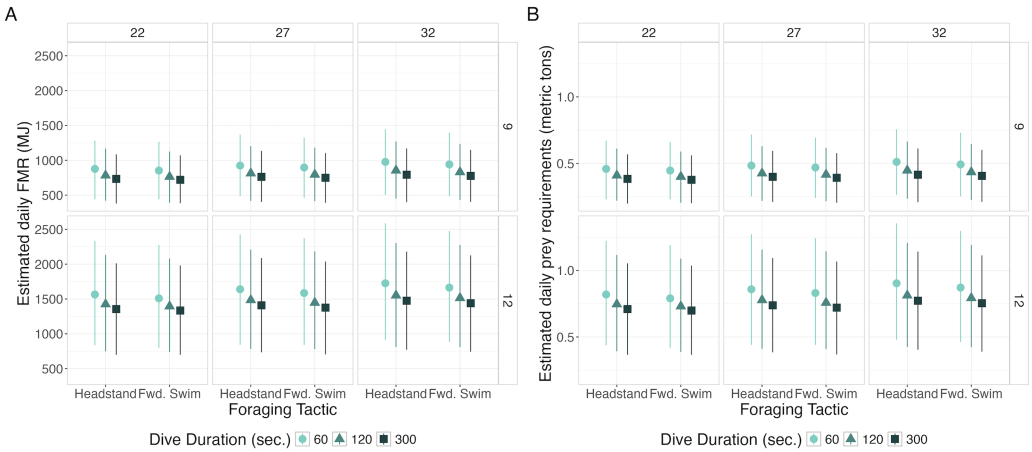

Figure 5 Estimated daily Field Metabolic Rate (FMR; MJ) (left) and prey requirements (metric tons) (right) from simulation exercise. Foraging tactic is on the *x*-axis, plots are faceted by body area index (BAI) in columns and total length (TL) in rows, point shapes and colors represent foraging dive durations. Each point represents the mean of the simulated values, and the bars represent 95% of the distribution.
Full-size DOI: 10.7717/peerj.20247/fig-5

DISCUSSION

We found that the duration of preceding dives is more strongly related with the respiration of gray whales than the duration of following dives. The relationships between the respiration metrics and total length, body condition, and preceding dive duration were consistent in direction, while the foraging tactic effects were variable. Additionally, we found no notable relationship between swim speed and respiration rate during travel. Combined, these results provide valuable insights into the factors potentially influencing PCFG gray whale energetics in this shallow foraging niche, laying the foundation for future studies to examine the energetic consequences of disturbance and environmental change. Our work also illustrates the complementarity of drone and accelerometry tag data when used in tandem to capture different perspectives on animal behavior.

Our finding that respiration by foraging PCFG gray whales appears to be more strongly related with recovery from the previous dive rather than anticipation for the next dive provides an interesting contrast to respiration patterns of other cetaceans. The breathing rate of long-finned pilot whales (*Globicephala melas*) only correlated with the duration of the preceding dive, not the following dive (*Isojunno et al., 2018*), whereas total inhalation duration of humpback (*Megaptera novaeangliae*) and minke (*Balaenoptera acutorostrata*) whales only correlated to the following dive, not the preceding (*Nazario et al., 2022*). While we would expect similar respiration patterns among baleen whales, it is important to note that, in our study system, gray whales perform shallow dives (up to depth of ~20 m) in contrast to the studies of other baleen whales (mean depth ~45 m, max ~250 m; *Nazario et al., 2022*). Furthermore, we did not find any evidence of pre-dive hyperventilation, which has been described in humpback whales (*Dolphin, 1987b*) and bottlenose dolphins (*Tursiops truncatus*; *Ridgway, Scronce & Kanwisher, 1969*). Thus, our results indicate that

PCFG gray whales may not need to physiologically anticipate dives in this shallow foraging habitat.

We found an overarching relationship between total length (TL) and various respiration metrics of gray whales. As respiration serves as a proxy for metabolic rate (*Fahlman et al., 2016*) we interpret these patterns as the result of the combined positive correlation between basal metabolic rate (BMR; the baseline energetic requirements of an individual) and size (*Kleiber, 1975*; *He et al., 2023*) and increased costs of locomotion for a large animal in shallow habitat (*Bird et al., 2024b*). The positive relationship between TL and total inhalation duration indicates that tidal volume and oxygen consumption increase with TL, aligning with previous findings (*Kooyman, 1973*; *Wahrenbrock et al., 1974*; *Fahlman et al., 2018*; *Cauture et al., 2019*; *Sumich et al., 2023*). The positive relationship between TL and inter-breath interval (IBI) equates to a negative relationship between total length and respiration rate, and consequently heart rate (*Blawas et al., 2021*). Similar relationships have been documented in several cetacean species including gray whales (*Ponganis & Kooyman, 1999*) and odontocetes (*Blawas et al., 2021*; *Spina et al., 2024*). Though the relationship between TL and respiration rate during travel was weaker (the 95% credible interval crossed zero), there was an 84% estimated probability of a positive relationship, which is contradictory to the IBI results. One possible explanation could be that whales travel close to the surface where drag is higher (*Vogel, 2020*) and the locomotive cost of stroking increases with body mass (*Williams et al., 2017*); therefore, it is possible that the positive relationship between TL and respiration rate is reflecting an increased cost of travel for larger whales. As a result of the estimated relationship between TL and the respiration metrics, and the documented positive relationship between TL and tidal volume (V_T, Eq. (2); *Sumich et al., 2023*), field metabolic rate (FMR) was estimated to increase with TL. However, we did not account for the energetic cost of growth for the 9 m whale, hence the difference in FMR between the 9 and 12 m simulations is likely an overestimate (*Sumich, 2021*; *Adamczak et al., 2023*).

Across all the models, higher BAI was consistently associated with an increased energetic cost. BAI had a negative relationship with IBI and a positive relationship with total inhalation duration, inhalation accumulation rate, and respiration rate. Combined, this suggests that whales in higher body condition consume more oxygen at an increased rate. Given that these whales are foraging in shallow habitat (<20 m; *Bird et al., 2024a*) and that increased body condition is linked to increased buoyancy (*Nousek-McGregor et al., 2014*; *Aoki et al., 2021*), we posit that this positive effect of BAI on energy expenditure reflects the costs of buoyancy in this shallow habitat. Furthermore, while we have never observed exhalations before diving, our results support the hypothesis that PCFG gray whales foraging in shallow habitat with higher body condition use bubble blasts to reduce the costs of buoyancy (*Bird et al., 2024b*). While deep dives are costly to marine mammals because of the duration of the breath hold (*Scholander, 1940*; *Kooyman, 1973*), several studies have found that shallow dives can be more costly, because of the cost of working against buoyant force (*Ridgway, Scronce & Kanwisher, 1969*; *Dolphin, 1987b*; *Costa, 1988*; *Costa & Gales, 2000*). The FMR simulation results showed that daily FMR was higher for whales in higher body condition, although the effect size was small.

Table 5 **Summary of field metabolic rate (FMR) and prey requirement comparisons across simulations, controlling for all other variables.**

	Total Length (TL; m)		Body Area Index (BAI)		Dive Duration (s)			Foraging Tactic
	12–9	**27–22**	**32–22**	**32–27**	**120–300**	**60–120**	**60–300**	**Headstand–Fwd. Swim**
Cohen's *d*	2.26 (0.07)***	0.17 (0.03)	0.36 (0.04)*	0.19 (0.02)	0.23 (0.04)*	0.44 (0.07)*	0.67 (0.10)***	0.11 (0.03)
Difference in FMR (MJ/day)	669.51 (37.14)	47.48 (16.76)	102.28 (35.34)	54.79 (19.13)	61.26 (12.06)	124.83 (26.3)	186.09 (37.99)	31.11 (14.38)
Difference in prey requirements (metric tons)	0.33 (0.02)	0.02 (0.01)	0.05 (0.02)	0.03 (0.01)	0.03 (0.01)	0.07 (0.01)	0.10 (0.02)	0.02 (0.01)

Notes.

The first row contains Cohen's d values. The next two rows contain the contrasts of FMR and prey requirements per comparison. All values are shown as mean (SD).

***Indicates a large effect size (>0.8).

**Indicates a moderate effect size (> 0.5).

*Indicates a small effect size (> 0.2).

Increased dive duration was associated with increased total inhalation duration, inhalation accumulation slope and breath count, and decreased IBI. Similar results have been found in many marine mammal species including pinnipeds (*Hindell & Lea, 1998*; *Williams et al., 2004*), odontocetes (*Isojunno et al., 2018*), and mysticetes (*Wursig, Wells & Croll, 1986*; *Dolphin, 1987b*; *Sumich, 2001*; *Keen & Qualls, 2018*). Contrastingly, the FMR simulation showed that shorter dives were more energetically expensive on a daily scale. This result may be due to the simulation design, where the simulated whale only dove using a single dive duration and kept diving until the total foraging time for the day was filled. Therefore, a simulated whale using 60 s dives dove more during one day than a whale using 300 s dives. However, recovery time did not increase with a 1:1 ratio. Rather, recovering from a single 300 s dive required less time than the total time needed to recover from five 60 s dives. As a result, over time it may be more energetically efficient to perform fewer long dives than many short dives. Such longer dives could also be more beneficial if they result in more intense bradycardia (*Thompson & Fedak, 1993*). While we chose to control dive duration in the simulations to compare our explanatory variables, future efforts should simulate a realistic mix of dive durations to more accurately estimate the daily FMR of foraging gray whales. More realistic estimates of FMR should also account for a potential diel bias in the activity budget from *Colson et al. (2024)*, which is based on tag data collected primarily during daytime. Further, as our FMR simulations were specifically designed to compare fixed effects on a daily scale, more realistic estimates of FMR that incorporate more variability in gray whale physiology and behavior would enable meaningful comparison with FMR estimates for other species.

The relationships between the different foraging tactics and the respiration metrics were variable. Headstanding and the forward swimming tactics appear to be more expensive as they had similarly high total inhalation durations, particularly in contrast to the surface tactics. The surface tactics occur just below the surface; therefore, the whale can easily surface as it is feeding. In the tag-based breath count model, the forward swimming tactics had a notably higher breath count than headstands and benthic digs, which is a surprising result considering *Colson (2023)* found that stroke rate is significantly higher during headstands. The FMR simulation results, based on the results of the respiration models, showed no notable difference between the headstanding and forward swimming tactics. Interestingly, *Colson (2023)* and *Bird et al. (2024a)* both found that headstanding and the forward swimming tactics are the most common tactics performed by PCFG gray whales and are relatively costly compared to the other tactics, suggesting that whales are able to capture sufficient prey to make using these tactics profitable (*Emlen, 1966*). Therefore, while the ontogenetic shift from forward swimming to headstanding (*Bird et al., 2024a*) may not be driven by different energetic costs of the tactics themselves, there may be increased costs associated with increased TL; perhaps headstanding provides longer individuals continued access to more profitable prey that also sustains the increased costs associated with length. Furthermore, headstanding may require time for learning and muscle development associated with growth (*Bird et al., 2024a*). Headstanding dives tend to be longer than forward swimming dives (*Bird et al., 2024b*), so headstanding may be more expensive *via* its relationship with dive duration, but our sample size was not

sufficient to explore this interaction. Future studies investigating how the interactions between morphology, behavior, stroke rate, and dive duration affect energetics will further clarify this hypothesis.

Bubble blasts had no notable effects on the respiration metrics (the 95% credible interval crossed 0). This result was not anticipated as bubble blasts are hypothesized to reduce the energetic cost of working against buoyant forces (*Bird et al., 2024b*). However, bubble blasts increase dive duration by ∼20 s during the stationary tactics (headstands and side-swim stationary; *Bird et al., 2024b*). Therefore, the effect of bubble blasts may manifest through its effect on dive duration rather than on respiration. Furthermore, the lack of detectable relationships could indicate that the bubble blast itself does not cost the whale additional energy due to the exhalation. Bubble blasts typically occur 20-30 s following the terminal inhalation, perhaps after oxygen extraction, meaning the whale does not need to inhale additional air for a bubble blast (*Sumich, 2001*).

Regarding the travel state, similar to *Mallonee (1991)* and *Stelle, Megill & Kinzel (2008)*, we found that IBIs during travel were longer than those during foraging, indicating that travel is less energetically costly than foraging. Furthermore, building on the work of *Sumich (1983)*, we expected to find a positive relationship between swim speed and respiration rate. However, we found no notable relationship between swim speed and respiration rate in either the drone or tag-based models. A factor to consider is that the whales in this study were travelling through a foraging ground, while *Sumich (1983)* observed whales on the south-bound migration. Therefore, there may be extra energetic costs of travel on a foraging ground that are unaccounted for here, such as digestion (*Williams et al., 2004*). Our sample size was also relatively small for travelling whales, as drone focal follows are limited to <15 min. A greater sample size could better inform our understanding of the cost of travel during the foraging season.

The limited flight time of the drone is a primary limitation of this study as it reduced the number of complete surface sequences we were able to observe. Limited visibility from the drone, either when the whale dove too deep or the water visibility was poor, also challenged the pilot's ability to follow the whale. However, the comparison of the drone and tag data showed that the drone data were not biased by beginning a focal follow at a random time within a foraging bout; there was no autocorrelation in the residuals of the tag breath count model, indicating that respiration between dives is independent. Our observed breath counts from drones (mean: 2.34, s.d: 1.95) and tags (mean: 3.42, s.d: 2.54) are similar to those reported for foraging gray whales off of British Columbia, Canada (mean: 2.47, s.d: 1.16; *Stelle, Megill & Kinzel, 2008*), St. Lawrence Island in the Bering Sea (mean: 4.27, s.d: 2.67; *Wursig, Wells & Croll, 1986*), and northern California, USA (mean: 3.52, s.d: 1.90; *Mallonee, 1991*).

We have shown here the power of pairing drone and tag data. The drone provided high resolution respiration metrics and high individual replicates across seven years, while the tag data provided better temporal coverage over a limited range of hours and individuals. Furthermore, the slight under- and over-dispersion of the respective drone and tag breath-count models provide an interesting contrast of the two methods. The under-dispersion of the drone model may reflect the limited observation duration, which

could result in an inflated proportion of shorter sequences. In contrast, the over-dispersion of the tag model may reflect the ability of the method to record the rarer occurrence of long sequences, with large breath counts, but on a limited number of individuals. By using these tools in tandem, we can continue to improve our understanding of respiration and energetics in free swimming large whales that are inaccessible using traditional methods.

We quantified respiration patterns using an established metric, inter-breath interval (IBI; *Wursig, Wells & Croll, 1986*; *Dolphin, 1987a*; *Stelle, Megill & Kinzel, 2008*) and novel metrics: total inhalation duration and inhalation accumulation rate. Our derived total inhalation duration metric serves as an improvement on breath count that incorporates breath-by-breath variability and estimates the total tidal volume of oxygen acquired during a surface sequence. The rate of inhalation accumulation metric integrates both total inhalation duration and IBI to reflect changes in both tidal volume and respiration rate, similar to minute volume (*Kooyman, 1973*).

There were no clear relationships between either the initial or terminal breaths with body size, condition, or dive duration. This result suggests that there is no recovery from or anticipation for a dive on the single breath scale in terms of tidal volume. The initial and terminal breath duration models had some of the highest individual-level random effect values, suggesting that some other individual level attribute might help explain this variability. We similarly found no difference in nares area by breath type, in contrast to *Nazario et al. (2022)*'s findings correlating the terminal breath area and duration to the following dive duration. Therefore, like the variability in individual breath durations, there is also unexplained variability in the nares area that needs to be further explored.

CONCLUSIONS

In conclusion, we found that TL had a large positive effect on energetic expenditure at the dive and daily scales and dive duration had a large positive effect at the dive scale but negative effect at the daily scale. BAI had a moderate positive effect on energetic costs at the dive and daily scales, and tactic use had a negligible effect. With these findings, we provide a foundation for future studies to estimate the energetic consequences of environmental change or anthropogenic disturbance with reduced uncertainty by using breath-by-breath metrics and accounting for individual morphology, body condition, and behavior. PCFG gray whales forage in near shore habitat where they are frequently exposed to vessel traffic, noise, and changing environmental conditions (*Hildebrand et al., 2022*; *Hildebrand et al., 2024*). While behavioral and physiological responses to these stressors have been documented (*Lemos et al., 2022*; *Pirotta et al., 2023*; *Pirotta et al., 2024*), the energetic consequences have not been quantified to date, which are needed to fully assess the population level impacts of these anthropogenetic activities. Our results contribute to our understanding of respiration and energetics in baleen whales and highlight the importance of studying the energetic consequences of shallow foraging. Given that the costs associated with buoyancy are highest in large whales, these results suggest that PCFG gray whales may be smaller and skinner than their ENP counterparts (*Torres et al., 2022*; *Bierlich et al., 2023*) because of an upper limit on size after which shallow diving becomes

too energetically expensive to be beneficial. If body condition is limited by buoyancy costs in this habitat, it could lead to decreased calving rates if females cannot build sufficient reserves to sustain pregnancy, ultimately leading to population-level effects (*Blueweiss et al., 1978*; *Stewart et al., 2022*; *Pirotta et al., 2025*). However, it is worth noting that here we focus on short-term foraging costs, but the impact on an individual's annual energy budget will be dependent on foraging success and rates of energy accumulation across longer time frames, which may be differentially affected by body size. Close and long-term monitoring of PCFG gray whale population dynamics, including vital rates, is needed to examine this hypothesis.

While the PCFG represents a rare example of a baleen whale primarily foraging in shallow habitat, the dynamic relationship between body condition and FMR suggests that the energetic cost of foraging should be estimated at multiple time points in a foraging season. Furthermore, these buoyancy related costs likely affect other species as well. Shallow prey patches have been hypothesized to be profitable for foraging cetaceans due to the shorter travel time required to reach them (*Doniol-Valcroze et al., 2011*). However, *Nichols et al. (2022)* found a decrease in number of humpback whale shallow foraging dives throughout the foraging season and several studies have documented a cessation of foraging at night when zooplankton prey vertically migrate to the surface (*Goldbogen et al., 2011*; *Burrows et al., 2016*; *Nickels, Sala & Ohman, 2019*). These studies hypothesized that this lack of shallow foraging was due to decreased density of prey near the surface; however, it is possible that the cost of shallow dives due to buoyancy also decreased the profitability of the prey. Consequently, our results suggest that the central place forager framework for baleen whales should be adjusted to incorporate the increased energetic expense of shallow diving as related to an individual's size and body condition. At shallow depths, assessment of an individual's buoyancy and energetic costs may elucidate variation in foraging decisions that cannot be explained by prey density alone.

ACKNOWLEDGEMENTS

We thank Todd Chandler, Hunter Warwick, Ines Hildebrand, Noah Goodwin-Rice, Kathryne Macallan, Ally Kane, Jen-Hsiu Ko, Ryan Giannelli, Abby Coffey, Wally Fiori, and Hali Peterson for assistance with data collection and processing. We thank Alyssa Thibodeau for providing guidance during analysis. We thank Mauricio Cantor and Tiffany Garcia for feedback on preliminary results.

ADDITIONAL INFORMATION AND DECLARATIONS

Funding

Data collection was supported by the NOAA National Marine Fisheries Service Office of Science and Technology Ocean Acoustics Program [2016 and 2017; 50-27], the Oregon Sea Grant Program Development funds [2018; RECO-40-PD], the Oregon State University Marine Mammal Institute [2019], and the Office of Naval Research Marine Mammals and Biology program [2020-2022; #N00014-20-1-2760]. The funders had no role in study design, data collection and analysis, decision to publish, or preparation of the manuscript.

Grant Disclosures

The following grant information was disclosed by the authors:
The NOAA National Marine Fisheries Service Office of Science and Technology Ocean Acoustics Program: 2016 and 2017; 50-27.
The Oregon Sea Grant Program Development funds: 2018; RECO-40-PD.
The Oregon State University Marine Mammal Institute [2019].
The Office of Naval Research Marine Mammals and Biology program: 2020-2022; # N00014-20-1-2760.

Competing Interests

The authors declare there are no competing interests.

Author Contributions

- Clara N. Bird conceived and designed the experiments, performed the experiments, analyzed the data, prepared figures and/or tables, authored or reviewed drafts of the article, and approved the final draft.
- Enrico Pirotta analyzed the data, authored or reviewed drafts of the article, and approved the final draft.
- Leslie New analyzed the data, authored or reviewed drafts of the article, and approved the final draft.
- Jamie M. Cornelius analyzed the data, authored or reviewed drafts of the article, and approved the final draft.
- James L. Sumich analyzed the data, authored or reviewed drafts of the article, and approved the final draft.
- Kate M. Colson performed the experiments, authored or reviewed drafts of the article, and approved the final draft.
- K.C. Bierlich performed the experiments, authored or reviewed drafts of the article, and approved the final draft.
- Lisa Hildebrand performed the experiments, authored or reviewed drafts of the article, and approved the final draft.
- Alejandro Apolo Fernández Ajó performed the experiments, authored or reviewed drafts of the article, and approved the final draft.
- Annie Doron performed the experiments, authored or reviewed drafts of the article, and approved the final draft.
- Leigh G. Torres conceived and designed the experiments, authored or reviewed drafts of the article, and approved the final draft.

Animal Ethics

The following information was supplied relating to ethical approvals (*i.e.*, approving body and any reference numbers):

Suction cup tagging was conducted under the IACUC approved for the Cascadia Research Collective.

Field Study Permissions

The following information was supplied relating to field study approvals (*i.e.*, approving body and any reference numbers):

Research was conducted under NOAA/NMFS permits 16011 and 21678. As the drone was in nadir and filming whales in the open ocean, humans were never recorded nor at risk of being recorded.

Data Availability

The following information was supplied regarding data availability:

The data is available at figshare: Bird, Clara (2025). Data and code for "Size and body condition drive the cost of foraging for a baleen whale in a shallow habitat". figshare. Journal contribution. https://doi.org/10.6084/m9.figshare.26999995.v1

Supplemental Information

Supplemental information for this article can be found online at http://dx.doi.org/10.7717/peerj.20247#supplemental-information.

REFERENCES

Adamczak SK, McHuron EA, Christiansen F, Dunkin R, McMahon CR, Noren S, Pirotta E, Rosen D, Sumich J, Costa DP. 2023. Growth in marine mammals: a review of growth patterns, composition and energy investment. *Conservation Physiology* **11**:coad035 DOI 10.1093/conphys/coad035.

Altmann J. 1974. Observational study of behavior: sampling methods. *Behaviour* **49**:227–266 DOI 10.1163/156853974X00534.

Aoki K, Isojunno S, Bellot C, Iwata T, Kershaw J, Akiyama Y, Martín López LM, Ramp C, Biuw M, Swift R, Wensveen PJ, Pomeroy P, Narazaki T, Hall A, Sato K, Miller PJO. 2021. Aerial photogrammetry and tag-derived tissue density reveal patterns of lipid-store body condition of humpback whales on their feeding grounds. *Proceedings of the Royal Society B: Biological Sciences* **288**:20202307 DOI 10.1098/rspb.2020.2307.

Bierlich KC, Hewitt J, Bird CN, Schick RS, Friedlaender A, Torres LG, Dale J, Goldbogen J, Read AJ, Calambokidis J, Johnston DW. 2021a. Comparing uncertainty associated with 1-, 2-, and 3D aerial photogrammetry-based body condition measurements of baleen whales. *Frontiers in Marine Science* **8**:1729 DOI 10.3389/fmars.2021.749943.

Bierlich KC, Kane A, Hildebrand L, Bird CN, Fernandez Ajo A, Stewart JD, Hewitt J, Hildebrand I, Sumich J, Torres LG. 2023. Downsized: gray whales using an alternative foraging ground have smaller morphology. *Biology Letters* **19**:20230043 DOI 10.1098/rsbl.2023.0043.

Bierlich KC, Schick R, Hewitt J, Dale J, Goldbogen J, Friedlaender A, Johnston D. 2021b. Bayesian approach for predicting photogrammetric uncertainty in morphometric measurements derived from drones. *Marine Ecology Progress Series* **673**:193–210 DOI 10.3354/meps13814.

Bierlich KC, Wengrove D, Bird CN, Davidson R, Chandler T, Torres LG, Cantor M. 2024. LidarBoX: a 3D-printed, open-source altimeter system to improve photogrammetric accuracy for off-the-shelf drones. *Drone Systems and Applications* **12**:1–10 DOI 10.1139/dsa-2023-0051.

Bird CN, Bierlich KC. 2020. CollatriX: a GUI to collate MorphoMetriX outputs. *Journal of Open Source Software* **5**:2328 DOI 10.21105/joss.02328.

Bird CN, Pirotta E, New L, Bierlich KC, Donnelly M, Hildebrand L, Fernandez Ajó A, Torres LG. 2024a. Growing into it: evidence of an ontogenetic shift in grey whale use of foraging tactics. *Animal Behaviour* **214**:121–135 DOI 10.1016/j.anbehav.2024.06.004.

Bird CN, Pirotta E, New L, Bierlich KC, Hildebrand L, Fernandez Ajó A, Torres LG. 2024b. Bubble blasts! An adaptation for buoyancy regulation in shallow foraging gray whales. *Ecology and Evolution* **14**:e70093 DOI 10.1002/ece3.70093.

Blawas AM, Nowacek DP, Rocho-Levine J, Robeck TR, Fahlman A. 2021. Scaling of heart rate with breathing frequency and body mass in cetaceans. *Philosophical Transactions of the Royal Society B: Biological Sciences* **376**:20200223 DOI 10.1098/rstb.2020.0223.

Blueweiss L, Fox H, Kudzma V, Nakashima D, Peters R, Sams S. 1978. Relationships between body size and some life history parameters. *Oecologia* **37**:257–272 DOI 10.1007/BF00344996.

Brown JH, Gillooly JF, Allen AP, Savage VM, West GB. 2004. Toward a metabolic theory of ecology. *Ecology* **85**:1771–1789 DOI 10.1890/03-9000.

Burnett JD, Lemos L, Barlow D, Wing MG, Chandler T, Torres LG. 2018. Estimating morphometric attributes of baleen whales with photogrammetry from small UASs: a case study with blue and gray whales. *Marine Mammal Science* **35**:108–139 DOI 10.1111/mms.12527.

Burrows JA, Johnston DW, Straley JM, Chenoweth EM, Ware C, Curtice C, De Ruiter SL, Friedlaender AS. 2016. Prey density and depth affect the fine-scale foraging behavior of humpback whales Megaptera novaeangliae in Sitka Sound, Alaska, USA. *Marine Ecology Progress Series* **561**:245–260 DOI 10.3354/meps11906.

Butler PJ, Woakes AJ. 1979. Changes in heart rate and respiratory frequency during natural behaviour of ducks, with particular reference to diving. *Journal of Experimental Biology* **79**:283–300 DOI 10.1242/jeb.79.1.283.

Calambokidis J, Pérez A. 2017. Internal recruitment to the PCFG from births to PCFG mothers. In: *Workshop on the status of North Pacific gray whales*. La Jolla: International Whaling Commission.

Calambokidis J, Perez A, Laake J. 2019. Updated analysis of abundance and population structure of seasonal gray whales in the Pacific Northwest, 1996–2017. Final report to NOAA. Seattle, Washington 1–72.

Cartwright R, Newton C, West KM, Rice J, Niemeyer M, Burek K, Wilson A, Wall AN, Remonida-Bennett J, Tejeda A, Messi S, Marcial-Hernandez L. 2016. Tracking the development of muscular myoglobin stores in mysticete calves. *PLOS ONE* **11**:e0145893 DOI 10.1371/journal.pone.0145893.

Cauture F, Sterba-Boatwright B, Rocho-Levine J, Harms C, Miedler S, Fahlman A. 2019. Using respiratory sinus arrhythmia to estimate inspired tidal volume in the bottlenose dolphin (*Tursiops truncatus*). *Frontiers in Physiology* **10**:128 DOI 10.3389/fphys.2019.00128.

Christiansen F, Rasmussen MH, Lusseau D. 2014. Inferring energy expenditure from respiration rates in minke whales to measure the effects of whale watching boat interactions. *Journal of Experimental Marine Biology and Ecology* **459**:96–104 DOI 10.1016/j.jembe.2014.05.014.

Christiansen F, Sprogis KR, Nielsen MLK, Glarou M, Bejder L. 2023. Energy expenditure of southern right whales varies with body size, reproductive state and activity level. *Journal of Experimental Biology* **226(12)**:jeb.245137 DOI 10.1242/jeb.245137.

Cohen J. 1988. *Statistical power analysis for the behavioral sciences*. New York: Routledge.

Colson KM. 2023. *Estimating the relative energetic cost of foraging in Pacific coast feeding group grey whales from biologging data*. Vancouver, British Columbia: University of British Columbia DOI 10.14288/1.0435623.

Colson KM, Pirotta E, New L, Cade DE, Calambokidis J, Bierlich KC, Bird CN, Ajó AF, Hildebrand L, Trites AW, Torres LG. 2024. Using accelerometry tags to quantify gray whale foraging behavior. *Marine Mammal Science* **41(2)**:313210 DOI 10.1111/mms.13210.

Cooke SJ, Blumstein DT, Buchholz R, Caro T, Fernández-Juricic E, Franklin CE, Metcalfe J, O'Connor CM, St. Clair CC, Sutherland WJ, Wikelski M. 2014. Physiology, behavior, and conservation. *Physiological and Biochemical Zoology: Ecological and Evolutionary Approaches* **87**:1–14 DOI 10.1086/671165.

Costa DP. 1988. Methods for studying the energetics of freely diving animals. *Canadian Journal of Zoology* **66**:45–52 DOI 10.1139/z88-006.

Costa DP, Gales NJ. 2000. Foraging energetics and diving behavior of lactating New Zealand Sea Lions, *Phocarctos Hookeri*. *Journal of Experimental Biology* **203**:3655–3665 DOI 10.1242/jeb.203.23.3655.

Darling JD, Keogh KE, Steeves TE. 1998. Gray whale (*Eschrichtius robustus*) habitat utilization and prey species off Vancouver Island, B.C.. *Marine Mammal Science* **14**:692–720 DOI 10.1111/j.1748-7692.1998.tb00757.x.

Dawson SM, Bowman MH, Leunissen E, Sirguey P. 2017. Inexpensive aerial photogrammetry for studies of whales and large marine animals. *Frontiers in Marine Science* **4**:366 DOI 10.3389/fmars.2017.00366.

DeRuiter S, Johnsom M, Sweeney D, Macnamara-Oh Y, Fynewever S, Tejevbo, Marques T, Wang Y, Ogedegbe. 2024. tagtools: work with data from high-resolution biologging tags. *Available at https://animaltags.github.io/tagtools_r/index.html*.

Dolphin WF. 1987a. Ventilation and dive patterns of humpback whales, *Megaptera novaeangliae*, on their Alaskan feeding grounds. *Canadian Journal of Zoology* **65**:83–90 DOI 10.1139/z87-013.

Dolphin WF. 1987b. Dive behavior and estimated energy expenditure of foraging humpback whales in southeast Alaska. *Canadian Journal of Zoology* **65**:354–362 DOI 10.1139/z87-055.

Domning DP, De Buffrénil V. 1991. Hydrostasis in the Sirenia: quantitative data and functional interpretations. *Marine Mammal Science* **7**:331–368 DOI 10.1111/j.1748-7692.1991.tb00111.x.

Doniol-Valcroze T, Lesage V, Giard J, Michaud R. 2011. Optimal foraging theory predicts diving and feeding strategies of the largest marine predator. *Behavioral Ecology* **22**:880–888 DOI 10.1093/beheco/arr038.

Dunham JS, Duffus DA. 2001. Foraging patterns of gray whales in central Clayoquot Sound, British Columbia, Canada. *Marine Ecology Progress Series* **223**:299–310 DOI 10.3354/meps223299.

Eguchi T, Lang A, Weller D. 2024. NOAA technical memorandum NMFS-SWFSC 695. Washington, D.C.: NOAA DOI 10.25923/N5QA-0Y54.

Emlen JM. 1966. The role of time and energy in food preference. *The American Naturalist* **100**:611–617 DOI 10.1086/282455.

Fahlman A, Brodsky M, Wells R, McHugh K, Allen J, Barleycorn A, Sweeney JC, Fauquier D, Moore M. 2018. Field energetics and lung function in wild bottlenose dolphins, *Tursiops truncatus*, in Sarasota Bay Florida. *Royal Society Open Science* **5(1)**:171280 DOI 10.1098/rsos.171280.

Fahlman A, Svärd C, Rosen DAS, Jones DR, Trites AW. 2008a. Metabolic costs of foraging and the management of O2 and CO2 stores in Steller sea lions. *Journal of Experimental Biology* **211**:3573–3580 DOI 10.1242/jeb.023655.

Fahlman A, Van der Hoop J, Moore MJ, Levine G, Rocho-Levine J, Brodsky M. 2016. Estimating energetics in cetaceans from respiratory frequency: why we need to understand physiology. *Biology Open* **5**:436–442 DOI 10.1242/bio.017251.

Fahlman A, Wilson R, Svärd C, Rosen DAS, Trites AW. 2008b. Activity and diving metabolism correlate in Steller sea lion *Eumetopias jubatus*. *Aquatic Biology* **2**:75–84 DOI 10.3354/ab00039.

Friard O, Gamba M. 2016. BORIS: a free, versatile open-source event-logging software for video/audio coding and live observations. *Methods in Ecology and Evolution* **7**:1325–1330 DOI 10.1111/2041-210X.12584.

Gelman A, Goodrich B, Gabry J, Vehtari A. 2019. R-squared for bayesian regression models. *The American Statistician* **73**:307–309 DOI 10.1080/00031305.2018.1549100.

Génin A, Richard G, Jouma'a J, Picard B, El Ksabi N, Vacquié Garcia J, Guinet C. 2015. Characterization of postdive recovery using sound recordings and its relationship to dive duration, exertion, and foraging effort of southern elephant seals (*Mirounga leonina*). *Marine Mammal Science* **31**:1452–1470 DOI 10.1111/mms.12235.

Goldbogen JA, Calambokidis J, Oleson E, Potvin J, Pyenson ND, Schorr G, Shadwick RE. 2011. Mechanics, hydrodynamics and energetics of blue whale lunge feeding: efficiency dependence on krill density. *Journal of Experimental Biology* **214**:131–146 DOI 10.1242/jeb.048157.

Halsey LG, Shepard ELC, Hulston CJ, Venables MC, White CR, Jeukendrup AE, Wilson RP. 2008. Acceleration *versus* heart rate for estimating energy expenditure and speed during locomotion in animals: tests with an easy model species, Homo sapiens. *Zoology* **111**:231–241 DOI 10.1016/j.zool.2007.07.011.

Harris J, Calambokidis J, Perez A, Mahoney PJ. 2022. *Recent trends in the abundance of seasonal gray whales (Eschrichtius robustus) in the Pacific Northwest, 1996–2022*. Seattle: Alaska Fisheries Science Center NOAA, National Marine Fisheries Service.

He RS, De Ruiter S, Westover T, Somarelli JA, Blawas AM, Dayanidhi DL, Singh A, Steves B, Driesinga S, Halsey LG, Fahlman A. 2023. Allometric scaling of metabolic rate and cardiorespiratory variables in aquatic and terrestrial mammals. *Physiological Reports* **11**:e15698 DOI 10.14814/phy2.15698.

Hildebrand L, Bernard KS, Torres LG. 2021. Do gray whales count calories? Comparing energetic values of gray whale prey across two different feeding grounds in the Eastern North Pacific. *Frontiers in Marine Science* **8**:683634 DOI 10.3389/fmars.2021.683634.

Hildebrand L, Derville S, Hildebrand I, Torres LG. 2024. Exploring indirect effects of a classic trophic cascade between urchins and kelp on zooplankton and whales. *Scientific Reports* **14**:9815 DOI 10.1038/s41598-024-59964-x.

Hildebrand L, Sullivan F, Orben R, Derville S, Torres LG. 2022. Trade-offs in prey quantity and quality in gray whale foraging. *Marine Ecology Progress Series* **695**:189–202 DOI 10.3354/meps14115.

Hindell MA, Lea M. 1998. Heart rate, swimming speed, and estimated oxygen consumption of a free-ranging southern elephant seal. *Physiological Zoology* **71**:74–84 DOI 10.1086/515890.

Houston AI, McNamara JM. 1985. A general theory of central place foraging for single-prey loaders. *Theoretical Population Biology* **28**:233–262 DOI 10.1016/0040-5809(85)90029-2.

Irving L. 1939. Respiration in diving mammals. *Physiological Reviews* **19**:112–134 DOI 10.1152/physrev.1939.19.1.112.

Isojunno S, Aoki K, Curé C, Kvadsheim PH, Miller PJO. 2018. Breathing patterns indicate cost of exercise during diving and response to experimental sound exposures in long-finned pilot whales. *Frontiers in Physiology* **9**:1462 DOI 10.3389/fphys.2018.01462.

Keen EM, Qualls KM. 2018. Respiratory behaviors in sympatric rorqual whales: the influence of prey depth and implications for temporal access to prey. *Journal of Mammalogy* **99**:27–40 DOI 10.1093/jmammal/gyx170.

Kleiber M. 1961. *The fire of life; an introduction to animal energetics*. New York: Wiley.

Kleiber M. 1975. Metabolic turnover rate: a physiological meaning of the metabolic rate per unit body weight. *Journal of Theoretical Biology* **53**:199–204 DOI 10.1016/0022-5193(75)90110-1.

Kooyman GL. 1973. Respiratory adaptations in marine mammals. *American Zoologist* **13**:457–468 DOI 10.1093/icb/13.2.457.

Kooyman GL, Norris KS, Gentry RL. 1975. Spout of the gray whale: its physical characteristics. *Science* **190**:908–910 DOI 10.1126/science.190.4217.908.

Kooyman GL, Ponganis PJ. 1998. The physiological basis of diving to depth: birds and mammals. *Annual Review of Physiology* **60**:19–32 DOI 10.1146/annurev.physiol.60.1.19.

Lang AR, Calambokidis J, Scordino J, Pease VL, Klimek A, Burkanov VN, Gearin P, Litovka DI, Robertson KM, Mate BR, Jacobsen JK, Taylor BL. 2014. Assessment of genetic structure among eastern North Pacific gray whales on their feeding grounds. *Marine Mammal Science* **30**:1473–1493 DOI 10.1111/mms.12129.

Lemos LS, Haxel JH, Olsen A, Burnett JD, Smith A, Chandler TE, Nieukirk SL, Larson SE, Hunt KE, Torres LG. 2022. Effects of vessel traffic and ocean noise on gray whale stress hormones. *Scientific Reports* **12**:18580 DOI 10.1038/s41598-022-14510-5.

Lovvorn JR, Jones DR. 1991. Effects of body size, body fat, and change in pressure with depth on buoyancy and costs of diving in ducks (*Aythya* spp.). *Canadian Journal of Zoology* **69**:2879–2887 DOI 10.1139/z91-406.

Mallonee JS. 1991. Behaviour of gray whales (*Eschrichtius robustus*) summering off the northern California coast, from Patrick's point to crescent City. *Canadian Journal of Zoology* **69**:681–690 DOI 10.1139/z91-100.

McElreath R. 2020. *Statistical rethinking: a Bayesian course with examples in R and Stan*. Boca Raton, Florida: CRC Press.

McRae TM, Volpov BL, Sidrow E, Fortune SME, Auger-Méthé M, Heckman N, Trites AW. 2024. Killer whale respiration rates. *PLOS ONE* **19**:e0302758 DOI 10.1371/journal.pone.0302758.

Nakagawa S, Schielzeth H. 2013. A general and simple method for obtaining R2 from generalized linear mixed-effects models. *Methods in Ecology and Evolution* **4**:133–142 DOI 10.1111/j.2041-210x.2012.00261.x.

Nazario EC, Cade DE, Bierlich KC, Czapanskiy MF, Goldbogen JA, Kahane-Rapport SR, Van der Hoop JM, Luis MTS, Friedlaender AS. 2022. Baleen whale inhalation variability revealed using animal-borne video tags. *PeerJ* **10**:e13724 DOI 10.7717/peerj.13724.

Nerini M. 1984. A review of gray whale feeding ecology. In: Jones ML, Swartz SL, Leatherwood S, eds. *The gray whale: Eschrichtius robustus*. Orlando, Florida: Academic Press, 423–450.

Nichols RC, Cade DE, Kahane-Rapport S, Goldbogen J, Stimpert A, Nowacek D, Read AJ, Johnston DW, Friedlaender A. 2022. Intra-seasonal variation in feeding rates and diel foraging behaviour in a seasonally fasting mammal, the humpback whale. *Royal Society Open Science* **9**:211674 DOI 10.1098/rsos.211674.

Nickels CF, Sala LM, Ohman MD. 2019. The euphausiid prey field for blue whales around a steep bathymetric feature in the southern California current system. *Limnology and Oceanography* **64**:390–405 DOI 10.1002/lno.11047.

Noren SR, Williams TM. 2000. Body size and skeletal muscle myoglobin of cetaceans: adaptations for maximizing dive duration. *Comparative Biochemistry and Physiology Part A: Molecular & Integrative Physiology* **126**:181–191 DOI 10.1016/S1095-6433(00)00182-3.

Nousek-McGregor AE, Miller CA, Moore MJ, Nowacek DP. 2014. Effects of body condition on buoyancy in endangered north atlantic right whales. *Physiological and Biochemical Zoology* **87**:160–171 DOI 10.1086/671811.

Olsen CR, Hale FC, Elsner R. 1969. Mechanics of ventilation in the pilot whale. *Respiration Physiology* **7**:137–149 DOI 10.1016/0034-5687(69)90001-2.

Pirotta E, Bierlich KC, New L, Hildebrand L, Bird CN, Fernandez Ajó A, Torres LG. 2024. Modeling individual growth reveals decreasing gray whale body length and correlations with ocean climate indices at multiple scales. *Global Change Biology* **30**:e17366 DOI 10.1111/gcb.17366.

Pirotta E, Booth CG, Costa DP, Fleishman E, Kraus SD, Lusseau D, Moretti D, New LF, Schick RS, Schwarz LK, Simmons SE, Thomas L, Tyack PL, Weise MJ, Wells RS, Harwood J. 2018. Understanding the population consequences of disturbance. *Ecology and Evolution* **8**:9934–9946 DOI 10.1002/ece3.4458.

Pirotta E, Fernandez Ajó A, Bierlich K, Bird CN, Buck CL, Haver SM, Haxel JH, Hildebrand L, Hunt KE, Lemos LS, New L, Torres LG. 2023. Assessing variation in faecal glucocorticoid concentrations in gray whales exposed to anthropogenic stressors. *Conservation Physiology* **11**:coad082 DOI 10.1093/conphys/coad082.

Pirotta E, New L, Fernandez Ajó A, Bierlich KC, Bird CN, Buck CL, Hildebrand L, Hunt KE, Calambokidis J, Torres LG. 2025. Body size, nutritional state and endocrine state are associated with calving probability in a long-lived marine species. *Journal of Animal Ecology* **94(7)**:1422–1434 DOI 10.1111/1365-2656.70068.

Ponganis PJ, Kooyman GL. 1999. Heart rate and electrocardiogram characteristics of a young california gray whale (*Eschrichtius Robustus*)1. *Marine Mammal Science* **15**:1198–1207 DOI 10.1111/j.1748-7692.1999.tb00885.x.

Ponganis PJ, Williams CL. 2016. Chapter 2: oxygen stores and diving. In: *Marine mammal physiology: requisites for ocean living*. *CRC marine biology series*, Boca Raton: CRC Press, Taylor & Francis, Group.

R Core Team. 2024. R: a language and environment for statistical computing. Vienna: R Foundation for Statistical Computing. *Available at https://www.r-project.org*.

Ridgway SH, Scronce BL, Kanwisher J. 1969. Respiration and deep diving in the bottlenose porpoise. *Science* **166**:1651–1654 DOI 10.1126/science.166.3913.1651.

Roos MMH, Wu G-M, Miller PJO. 2016. The significance of respiration timing in the energetics estimates of free-ranging killer whales (*Orcinus orca*). *Journal of Experimental Biology* **219**:2066–2077 DOI 10.1242/jeb.137513.

Schoener TW. 1971. Theory of feeding strategies. *Annual Review of Ecology and Systematics* **2**:369–404 DOI 10.1146/annurev.es.02.110171.002101.

Scholander PF. 1940. Experimental investigations on the respiratory function in diving mammals and birds. *Hvalradets Skrifter* **22**:1–131.

Spina F, Weiss MN, Croft DP, Luschi P, Massolo A, Domenici P. 2024. The effect of formation swimming on tailbeat and breathing frequencies in killer whales. *Behavioral Ecology and Sociobiology* **78**:75 DOI 10.1007/s00265-024-03492-1.

Stan Development Team. 2020. RStan: the R interface to Stan. R package version 2.21.1. *Available at https:// mc-stan.org/*.

Stelle LL, Megill WM, Kinzel MR. 2008. Activity budget and diving behavior of gray whales (*Eschrichtius robustus*) in feeding grounds off coastal British Columbia. *Marine Mammal Science* **24**:462–478 DOI 10.1111/j.1748-7692.2008.00205.x.

Stephenson R, Lovvorn JR, Heieis MRA, Jones DR, Blake RW. 1989. A hydromechanical estimate of the power requirements of diving and surface swimming in lesser scaup (*Aythya Affinis*). *Journal of Experimental Biology* **147**:507–518 DOI 10.1242/jeb.147.1.507.

Stewart J, Durban J, Europe H, Fearnbach H, Hamilton P, Knowlton A, Lynn M, Miller C, Perryman W, Tao B, Moore M. 2022. Larger females have more calves: influence of maternal body length on fecundity in North Atlantic right whales. *Marine Ecology Progress Series* **689**:179–189 DOI 10.3354/meps14040.

Sumich JL. 1983. Swimming velocities, breathing patterns, and estimated costs of locomotion in migrating gray whales, Eschrichtius robustus. *Canadian Journal of Zoology* **61**:647–652 DOI 10.1139/z83-086.

Sumich JL. 2001. Direct and indirect measures of oxygen extraction, tidal lung volumes and respiratory rates in a rehabilitating gray whale calf. *Aquatic Mammals* **27**:279–283.

Sumich JL. 2021. Why Baja? A bioenergetic model for comparing metabolic rates and thermoregulatory costs of gray whale calves (*Eschrichtius robustus*). *Marine Mammal Science* **37(3)**:870–887 DOI 10.1111/mms.12778.

Sumich JL, Albertson R, Torres LG, Bird CN, Bierlich KC, Harris C. 2023. Using audio and UAS-based video for estimating tidal lung volumes of resting and active adult gray whales (*Eschrichtius robustus*). *Marine Mammal Science* **40(2)**:e13081 DOI 10.1111/mms.13081.

Sumich JL, May MA. 2009. Scaling and remote monitoring of tidal lung volumes of young gray whales, *Eschrichtius robustus*. *Marine Mammal Science* **25**:221–228 DOI 10.1111/j.1748-7692.2008.00272.x.

Thompson D, Fedak MA. 1993. Cardiac responses of grey seals during diving at sea. *Journal of Experimental Biology* **174**:139–154 DOI 10.1242/jeb.174.1.139.

Torres W, Bierlich KC. 2020. MorphoMetriX: a photogrammetric measurement GUI for morphometric analysis of megafauna. *Journal of Open Source Software* **5**:1825 DOI 10.21105/joss.01825.

Torres LG, Bird CN, Rodríguez-González F, Christiansen F, Bejder L, Lemos L, Urban RJ, Swartz S, Willoughby A, Hewitt J, Bierlich KC. 2022. Range-wide comparison of gray whale body condition reveals contrasting sub-population health characteristics and vulnerability to environmental change. *Frontiers in Marine Science* **9**:867258 DOI 10.3389/fmars.2022.867258.

Torres LG, Nieukirk SL, Lemos L, Chandler TE. 2018. Drone up! Quantifying whale behavior from a new perspective improves observational capacity. *Frontiers in Marine Science* **5**:319 DOI 10.3389/fmars.2018.00319.

Villegas-Amtmann S, Schwarz LK, Sumich JL, Costa DP. 2015. A bioenergetics model to evaluate demographic consequences of disturbance in marine mammals applied to gray whales. *Ecosphere* **6**:art183 DOI 10.1890/ES15-00146.1.

Vogel S. 2020. *Life in moving fluids: the physical biology of flow—revised and expanded*. Second edition. Princeton, New Jersey: Princeton University Press.

Wahrenbrock EA, Maruschak GF, Elsner R, Kenney DW. 1974. Respiration and metabolism in two baleen whale calves. *Marine Fisheries Review* **36**:3–9.

Williams TM. 1999. The evolution of cost efficient swimming in marine mammals: limits to energetic optimization. *Philosophical Transactions of the Royal Society B: Biological Sciences* **354**:193–201 DOI 10.1098/rstb.1999.0371.

Williams TM, Fuiman LA, Horning M, Davis RW. 2004. The cost of foraging by a marine predator, the Weddell seal *Leptonychotes weddellii*: pricing by the stroke. *Journal of Experimental Biology* **207**:973–982 DOI 10.1242/jeb.00822.

Williams TM, Fuiman LA, Kendall T, Berry P, Richter B, Noren SR, Thometz N, Shattock MJ, Farrell E, Stamper AM, Davis RW. 2015. Exercise at depth alters bradycardia and incidence of cardiac anomalies in deep-diving marine mammals. *Nature Communications* **6**:6055 DOI 10.1038/ncomms7055.

Williams TM, Kendall TL, Richter BP, Ribeiro-French CR, John JS, Odell KL, Losch BA, Feuerbach DA, Stamper MA. 2017. Swimming and diving energetics in dolphins: a stroke-by-stroke analysis for predicting the cost of flight responses in wild odontocetes. *Journal of Experimental Biology* **220**:1135–1145 DOI 10.1242/jeb.154245.

Williams R, Noren DP. 2009. Swimming speed, respiration rate, and estimated cost of transport in adult killer whales. *Marine Mammal Science* **25**:327–350 DOI 10.1111/j.1748-7692.2008.00255.x.

Winship AJ, Trites AW, Rosen DAS. 2002. A bioenergetic model for estimating the food requirements of Steller sea lions *Eumetopias jubatus* in Alaska, USA. *Marine Ecology Progress Series* **229**:291–312 DOI 10.3354/meps229291.

Wursig B, Wells RS, Croll DA. 1986. Behavior of gray whales summering near St. Lawrence Island, Bering Sea. *Canadian Journal of Zoology* **64**:611–621 DOI 10.1139/z86-091.